Ultrafast Processes: Coordination Chemistry and Quantum Theory

Chantal Daniel

▶ **To cite this version:**

Chantal Daniel. Ultrafast Processes: Coordination Chemistry and Quantum Theory. Physical Chemistry Chemical Physics, 2020, 23 (1), pp.43-58. 10.1039/D0CP05116K . hal-03034533

HAL Id: hal-03034533
https://hal.science/hal-03034533

Submitted on 9 Nov 2021

HAL is a multi-disciplinary open access archive for the deposit and dissemination of scientific research documents, whether they are published or not. The documents may come from teaching and research institutions in France or abroad, or from public or private research centers.

L'archive ouverte pluridisciplinaire **HAL**, est destinée au dépôt et à la diffusion de documents scientifiques de niveau recherche, publiés ou non, émanant des établissements d'enseignement et de recherche français ou étrangers, des laboratoires publics ou privés.

HAL
archives-ouvertes.fr

Ultrafast Processes: Coordination Chemistry and Quantum Theory

Chantal Daniel

▶ To cite this version:

Chantal Daniel. Ultrafast Processes: Coordination Chemistry and Quantum Theory. Physical Chemistry Chemical Physics, Royal Society of Chemistry, 2020, 23 (1), pp.43-58. 10.1039/D0CP05116K . hal-03034533

HAL Id: hal-03034533
https://hal.archives-ouvertes.fr/hal-03034533

Submitted on 9 Nov 2021

HAL is a multi-disciplinary open access archive for the deposit and dissemination of scientific research documents, whether they are published or not. The documents may come from teaching and research institutions in France or abroad, or from public or private research centers.

L'archive ouverte pluridisciplinaire **HAL**, est destinée au dépôt et à la diffusion de documents scientifiques de niveau recherche, publiés ou non, émanant des établissements d'enseignement et de recherche français ou étrangers, des laboratoires publics ou privés.

PCCP

Ultrafast Processes: Coordination Chemistry and Quantum Theory

Journal:	*Physical Chemistry Chemical Physics*
Manuscript ID	Draft
Article Type:	Perspective
Date Submitted by the Author:	n/a
Complete List of Authors:	Daniel, Chantal; CNRS-Strasbourg University, Chemistry

SCHOLARONE™
Manuscripts

ARTICLE

Ultrafast processes: Coordination Chemistry and Quantum Theory

Chantal Daniel*[a]

Received 00th January 20xx,
Accepted 00th January 20xx

DOI: 10.1039/x0xx00000x

Coordination compounds characterized by fascinating and tunable electronic properties easily bind proteins, polymers, wires or DNA. Upon irradiation these molecular systems develop functions finding applications in solar cells, photocatalysis, luminescent and conformational probes, electron transfer triggers and diagnostic or therapeutic tools. The control of these functions is activated by the light wavelength, the metal/ligands cooperation and the environment within the first picoseconds (ps). After a brief summary of the theoretical background, this perspective reviews case studies, from 1st row to 3rd row transition metal complexes, that illustrate how spin-orbit, vibronic couplings and quantum effects drive the photophysics of this class of molecules at the early stage of the photoinduced elementary processes within the fs-ps time scale range.

1 Introduction

Electronic excited state decay in transition metal complexes started to be discussed in the 70's[1] in terms of radiative / non-radiative processes quantum yields and lifetimes. Very soon the role of intersystem crossing appeared to be very important on the basis of strong spin-orbit coupling (SOC) effects induced by the presence of heavy metal atoms.[2] The earlier studies were mainly dedicated to molecules with a long-lived triplet excited state responsible for phosphorescence, such as Ru(II), Pt(II) and Ir(III) complexes obtained by direct metalation of an organic chromophore[3] the bodipy being the most famous one.[4] Investigation of the radiative vs. non-radiative decay on the basis of Kasha, El-Sayed rules and energy gap law was the norm following the success of these early concepts at interpreting the photophysics of organic molecules on the basis of almost pure S_1/T_1 electronic states within a weak coupling limit (Scheme 1 (a)). This approach is still successful for coordination compounds specifically designed to avoid high density of nearly degenerate low-lying excited states, important nuclear relaxation, strong coupling and large electronic mixing.[5] The interpretation of the photophysics will be safely based on steady-state spectroscopies and single-determinant computational approaches focusing on the electronic and structural properties of the S_0 ground state and S_1/T_1 excited states[6] within either the metal-to-ligand-charge-transfer (MLCT) model or the intra-ligand (IL) model considering multi-step 100% ultrafast decay to S_1.[7] Refined zero magnetic field splitting studies varying the chemical environment, the temperature and the pressure can be performed for a quantitative assessment of SOC effects and a deep understanding of the photophysics.[8]

When designing coordination compounds for specific functions and applications the main concern is to tailor the photophysical properties by varying the metal center(s), the ligands and the environment in order to obtain large quantum yields and a palette of bright color's, efficient intersystem crossing (ISC) quantum yields, various kinetics and time-scales.[9] The probability to get back to the S_1/T_1 "ideal" situation described above allowing the use of simple techniques and concepts developed in the 60-70's for organic chromophores is very low. Indeed, most of the time the systems are characterized by a high density of excited states, nearly degenerate low-lying excited states of mixed character opening the route to a number of channels of deactivation of various time-scales before reaching the lowest long-lived T_1 state (Scheme 1(b)).

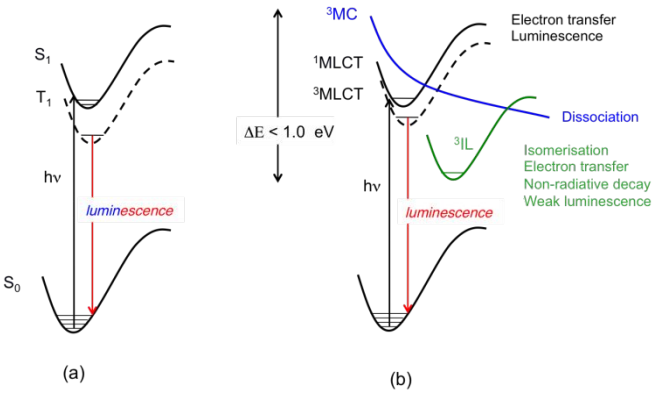

Laboratoire de Chimie Quantique Université de Strasbourg CNRS UMR7177
Institut Le Bel 4 Rue Blaise Pascal
67000 Strasbourg, France
e-mail : c.daniel@unistra.fr

† Footnotes relating to the title and/or authors should appear here.
Electronic Supplementary Information (ESI) available: [details of any supplementary information available should be included here]. See DOI: 10.1039/x0xx00000x

Scheme 1. (a) Luminescent decay based on the two-state model (b) Cartoon of typical radiative and non-radiative decays in coordination compounds.

Sophisticated time-resolved spectroscopies, sometimes supplemented by time-resolved X-ray absorption techniques, are mandatory to decipher the electronic excited state decays inherently linked to nuclear relaxation within ps-fs time-scales.[10]
This is illustrated by recent studies dedicated to 1st, 2nd and 3rd row transition metal complexes involved in chemical catalysis and biochemical processes,[11] in metal-based charge transfer chromophores,[12] phosphorescent materials for OLEDs,[13] photosensitizers and photocatalysts[14] or metallophilic oligomers designed for functional molecular assemblies and light-emitting devices.[15] Cu(I) complexes, seat of large photoinduced structural changes in the low-lying electronic excited states, have motivated a number of illuminating experimental and theoretical studies.[16]
The ultimate goal of this field of research is to control the excited state dynamics by means of tailored pulses that manipulate the vibrations of the molecules to regulate the population of the key electronic states for specific processes (luminescent decay, ultrafast electron transfer at long distances, selective dissociation, thermally activated delay fluorescence **(**TADF)…).[17]

In parallel theoretical investigations need robust highly correlated electronic structure theory able to determine the molecular structure of both ground and low-lying excited states and to describe on the same footing various electronic states, namely metal-centered (MC), MLCT, IL, ligand-to-ligand charge transfer (LLCT), ligand-to-metal charge transfer (LMCT) states of mixed character, relativistic, solvent and SOC effects. Ultimately, simulation of the evolution of the molecular states in real time by means of non-adiabatic quantum dynamics or semi-classical trajectories including SOC effects should give access to observables (time-resolved spectra, quantum yields, time-scales…).
This perspective based on recent research in the field of coordination chemistry is organized as follow: theoretical background is summarized in the next section with presentation of the most recent electronic structure methods available for providing excited state structures, transition energies, spin and vibronic couplings subsequently used in molecular dynamics or wavepacket simulations. Finally, case studies reporting the simulation of excited state non-adiabatic dynamics in 1st row to 3rd row transition metal complexes illustrate how spin-orbit, vibronic couplings and quantum effects drive the photophysics of this class of molecules at the early stage of the photoinduced elementary processes within the fs-ps time scale range.

2 Theoretical background

2.1 Electronic structure theory

2.1.1 Methods

Linear response time-dependent density functional theory (TD-DFT)[18] revolutionized computational coordination chemistry of excited state properties after decades of investigation based on configuration interaction (CI)[19] and multi-configuration self-consistent fied (MC-SCF)[20] derived approaches in an intent to model with more or less success the absorption spectra of simple transition metal complexes, struggling with appropriate "active" MO's (molecular orbitals) and electrons. Pioneering comparative studies put in evidence a curiously good agreement between complete active space (CASSCF)[21] / CAS-Perturbation theory 2nd order (CASPT2)[22] and TD-DFT results for Ru(II) complexes provided that TD-DFT includes solvent correction.[23] More recently a less optimistic conclusion about the ability of TD-DFT at reproducing the main features of the visible experimental absorption spectra of Re(I) complexes in water including SOC effects points out the difficulties at describing on the same footing the bands generated by MLCT, IL and LLCT transitions.[24] Recent advances within the multirefence wavefunction framework, such as restricted (RASSCF),[25] generalized (GASSCF),[26] split-GAS,[27] localized (LASSCF)[28] or occupied-restricted multiple (ORMAS)[29] techniques aim at reducing the exponential scaling of CASSCF-based methods leading to enlarged active spaces, beyond twenty electrons correlated in twenty active orbitals with more specific partition. LASSCF has been recently applied to predict spin-state energetics in mono- and di-iron complexes with accuracy comparable to CASSCF at a lower computational cost.[30] The ORMAS- formalism has been extended to a general spin-complete spin-flip CI method (SP-ORMAS-CI) including the computation of analytical gradient and non-adiabatic couplings.[31] This single determinant method, applied until now to organic molecules, reveals reasonably good agreement with standard multireference methods.
Density matrix renormalization group (DMRG) method[32] with more favorable scaling allows the inclusion of about hundred correlated electrons in hundred active orbitals. In it's automated version, based on iterative entanglement measures,[33] diagrammatic representation of the static correlation between each pair of orbitals and of how their occupation diverge from 0 or 2 facilitates the choice of the active space without any *a priori* in a black-box mode. Whereas CASPT2 calculations performed on top of limited CASSCF wavefunctions lead to results of limited value its extension to larger active space by using DMRG as solver gives quantitative results for transition metal complexes as shown recently.[34]

The drawbacks of TD-DFT in the context of excited state coordination chemistry are twofold: i) the electronic diversity and flexibility of this class of molecules hardly live with the approximations and limitations of the method; ii) applying solvent or relativistic corrections by approximate approaches within the framework of an approximate method may result in a total misunderstanding of the physics and prevents any robust interpretation both of the calculated properties and defects of the method itself. Whereas developing hundreds of more and more sophisticated functionals[35] may help at approaching a realistic solution for the ground state physical system the task would be titanic for the excited states because of this diversity.[36]

The next breakthrough will certainly come from excited state specific methods developed within an hybrid DFT/wavefunction formalism such as Multiconfiguration pair-DFT (MC-PDFT),[37] or DFT-multireference CI (DFT-MRCI).[38] Nevertheless, TD-DFT and satellite developments[39] are capable of treating a number of problems related to excited-state coordination chemistry and give most of the time appropriate qualitative insights. This makes the charm of the method provided that the conclusions have to be faced to reliable experimental data and/or accurate *ab initio* results with careful emphasis on the interpretation.[40]

This journal is © The Royal Society of Chemistry 20xx

Please do not adjust margins

2.1.2 Spin-orbit and vibronic couplings

Vibronic coupling theory has been developed in connection with a model Hamiltonian based on a diabatic representation of the electronic states.[41] The diabatic Hamiltonian describing η_{el} coupled electronic states is written as

$$H(Q) = \left(T_N + V_0(Q)\right)\mathrm{II} + W(Q)$$

Where T_N is the kinetic enery operator, $V(Q_0)$ is the potential energy of some reference electronic state, usually the electronic, ground state, II is the η_{el} x η_{el} identity matrix and $W(Q)$ is the coupling matrix that contains the electronic eigenvalues, the $\kappa_i^{(n)}$ intrastate and the $\lambda_i^{(nm)}$ inter-state vibronic couplings for n and m electronic states and i nuclear degree of freedom. The theory has been extended in order to include spin-orbit couplings in the formalism within the spin-vibronic concept.[42]

Most of the electronic structure theories described above provide electronic ground state to excited states transition energies, gradient of the energy, Hessian and SOC, critical data for the construction of the $W(Q)$ matrix.

Multiplet states, more particularly triplet states govern the photophysics of coordination compounds[43] SOC playing a key role in intersystem crossing, phosphorescence, TADF, singlet fission phenomena and magnetic properties.[44] At the TD-DFT level of theory SOC is perturbationally computed either within the relativistic two-component zero-order regular approximation ZORA scheme[45] or according to more sophisticated methods.[46] In multiconfiguration wavefunction approaches SOC is often included *a posteriori* based on the concept of interacting electronic states via SOC using part of the Douglas-Kroll Hamiltonian[47] within the one-electron effective Hamiltonian scheme.[48] A number of approximate SOC operators have been developed for practical use in molecular quantum chemistry and introduced either perturbationnally or variationally in electronic structure theory.[49]

The intrastate $\kappa_i^{(n)}$ and inter-state linear $\lambda_i^{(nm)}$ vibronic coupling constants generated by the vibrational molecular activity regulated by molecular symmetry rules are obtained by analytical formula when only two electronic states are involved within the linear vibronic coupling model.[41] The coupling constants can be deduced from electronic structure calculations using the first and second derivatives of the adiabatic potential energy surfaces $V_n(\boldsymbol{Q})$ with respect to Q_i at the ground state equilibrium geometry:

$$\kappa_i^{(n)} = \left.\frac{\partial V_n(\boldsymbol{Q})}{\partial Q_i}\right|_0$$

$$\lambda_i^{(nm)} = \left.\sqrt{\frac{1}{8}\frac{\partial^2 (V_m(\boldsymbol{Q}) - V_n(\boldsymbol{Q}))^2}{\partial Q_i^2}}\right|_0$$

Alternatively and in order to go beyond the pair of states approximation and the linear formalism, $\lambda_i^{(nm)}$can be computed on the basis of the overlap matrix between the electronic wavefunctions at close-lying geometries[50] as an adiabatic-to-diabatic transformation matrix, such that the linear vibronic coupling (LVC) constants can be obtained by means of numerical differentiation.

$$\lambda_i^{(n,m)} = \left.\frac{\partial}{\partial Q_i}\left\langle \Phi_n \middle| H_{el} \middle| \Phi_m \right\rangle\right|_0$$

The method is applicable to wavefunction-based methods as well as to TD-DFT. In the latter case the wavefunctions are replaced by auxiliary many-electron wavefunctions.[51] Quadratic vibronic coupling terms $\gamma_i^{(n)}$ and higher power terms may be added to the $W(Q)$ coupling matrix in order to describe the differences between ground- and excited state vibrational frequencies and to go beyond the harmonic approximation. [52]

2.2 Non-adiabatic dynamics: quantum vs. semi-classical

Two main approaches are available for simulating non-adiabatic dynamics, namely those using basis functions, intrinsically quantum and those based on trajectories mixing a classical picture of the nuclei with a quantum description of the electrons.

Since the original costly quantum method based on time-independent grid functions to solve the time-dependent nuclear Schrödinger equation[53] several approaches have been developed aiming at increasing the number of degrees of freedom included in the simulation for a broader applicability. The most popular one is based on time-dependent compact basis sets as implemented in the variational multiconfiguration time-dependent Hartree (MCTDH) method.[54] MCTDH and its multilayer extension[55] have been used, including up to fifteen normal modes, for simulating the ultrafast non-adiabatic decay of a number of Rhenium (I) complexes[56] as well as in the study of excited state dynamics of 1st-row transition metal complexes.[52,57]

In order to avoid the construction of full potential energy surfaces (PES), "on-the-fly" methods in which the potential energies are computed at the critical nuclear geometries by using localized traveling Gaussian basis functions, have been developed. The evolution of the basis functions can be driven either by an algorithm based on variational principle like in Gaussian-MCTDH (G-MCTDH),[58] variational multiconfiguration Gaussian (vMCG)[59] and direct-dynamics vMCG (DD-vMCG)[60] or by classical mechanics like in multiconfigurational Ehrenfest (MCE)[61], classical limit of G-MCTDH. In the *ab initio* multiple spawning (AIMS) approach[62] the Gaussian basis functions follow single-state forces but the basis set is expanded when the trajectory basis functions become sufficiently mixed. A variant, so-called *ab initio* multiple cloning (AIMC),[63] combining the best features of MCE and AIMS keeps the benefits of mean-field evolution during periods of strong non-adiabatic coupling while avoiding mean-field artifacts of the Ehrenfest dynamics. Ultrafast non-adiabatic chemistry of dimethylnitramine-Fe compound has been investigated by means of AIMS method.[64]

Whereas the above quantum methods are in principle exact within the dimensionality limits in terms of basis set and degrees of freedom the semi-classical methods described in the next section

have to be used with care when quantum effects control the excited state dynamics.

Mixed *quantum-classical* protocol based on classical point-like trajectories for the description of the nuclei and quantum-mechanical approaches for treating the electrons are an interesting alternative to fully quantum methods in the context of large molecular systems or when environment effects have to be taken into account. Indeed in principle all degrees of freedom are included and the dynamics can be coupled with quantum mechanics/ molecular mechanics (QM/MM) methods. In the most popular method, so-called trajectory surface hopping (TSH),[65] trajectories follow the gradient of the energy of one single electronic state, each trajectory being independent from the others. Despite of the limitations in terms of time-scale, number of trajectories and description of pure quantum effects (tunneling, de-coherences, interferences…) this efficient and simple method is widely used in chemistry, biology, and surface chemistry. It's extension to non-adiabatic dynamics including spin-orbit coupling[66] paved the way to challenging applications, including transition metal complexes.[67]

Recent implementation of the linear vibronic coupling (LVC) model, described in the previous section, within surface hoping approach[68] resulted in efficient feedback analysis of coherences and frequencies in non-adiabatic dynamics of large transition metal complexes.[69]

Quantum de-coherence induced by trajectory-based methods within a non-adiabatic coupling picture can be captured more or less rigorously depending on the level of approximation of the mixed quantum-classical protocol. One promising approach to deal with this problem, especially crucial for the study of photophysical and photochemical processes, is the coupled-trajectory mixed quantum-classical (CT-MQC) method based on the exact factorization of the total molecular wavefunction.[70] Its power lies in its capability at properly taking into account quantum de-coherence effects in the simulation of excited state dynamics in the full electronic and nuclear molecular dimensionality as illustrated by its application to the photochemistry of oxirane.[71] In this pioneering simulation trajectories adopt quantum wavepacket behaviors.

Further reading on the new representation of the non-Born-Oppenheimer problem through the handling of the full molecular wavefunction is referred to a recent review describing the different approaches within the context of quantum as well as mixed *quantum-classical* dynamics.[72]

Whereas the cost and accuracy of fully quantum dynamics methods will be controlled by the reduction of dimensionality and basis sets quality, a reduced number of trajectories, inappropriate initial conditions or de-coherence corrections and turn-on/off of the coupling activity on the fly can bias the results of quantum-classical methods. In both approaches the accuracy of the chosen electronic structure method is critical.

The next section gives some flavor of the current simulations in our quest for understanding and interpreting ultrafast excited state dynamics in a number of coordination compounds having the potential for efficient photosensitizers, photoswitches, thermally activated delay fluorescence materials, luminescent molecular probes or electron transfer triggers.

3 From 1st to 3rd-row transition metal complexes

3.1 Ultrafast decay in Iron(II) and Ru(II) complexes

Since the discovery of the light-induced excited spin-state trapping (LIESST)[73] ultrafast decay within the singlet/triplet/quintet manifold of spin-crossover Fe(II) complexes has fascinated experimentalists as well as theoreticians. Whereas both $[Ru(bpy)_3]^{2+}$ and $[Fe(bpy)_3]^{2+}$ are the seat of ultrafast intersystem crossings[74] the 2nd-row complex gets trapped into a long-lived ^{3}MLCT excited state suitable for photosensitizing and photocatalysis while the ecologically compatible 1st-row compound relaxes into the non-emissive ^{5}MC state within less than 100 fs preventing photovoltaic applications. Exploiting ligand properties for tailoring the MLCT/MC ordering in transition metal complexes is one standard tool of coordination chemistry. By substituting the bipyridine ligands by strongly σ-donor N-heterocyclic carbene (NHC) in $[Fe(bmip)_2]^{2+}$ (bmip = 2,6-bis(3-methyl-imidazole-1-ylidine)-pyridine) Liu et al[75], have paved the way to long-lived triplet MLCT states in iron complexes[76] up to ~ 2 ns lifetime.

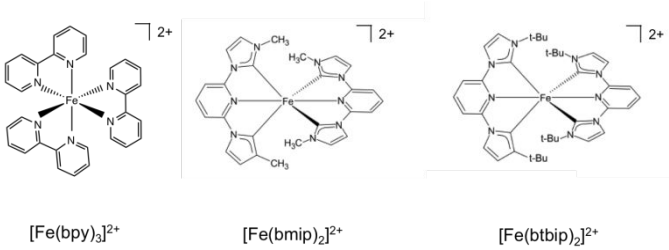

$[Fe(bpy)_3]^{2+}$ $[Fe(bmip)_2]^{2+}$ $[Fe(btbip)_2]^{2+}$

Figure 1. Schematic structures of $[Fe(bpy)_3]^{2+}$, $[Fe(bmip)_2]^{2+}$ and $[Fe(btbip)_2]^{2+}$ complexes.

Iron(II) complexes. Electronic structure calculations performed at the MS-CASPT2 and TD-DFT levels for $[Fe(bpy)_3]^2$ and $[Fe(bmip)_2]^{2+}$[57d,77], respectively, confirm a destabilization of the MC states in the bmip substituted complex preventing the population of the lowest $^5T_2$ quintet state in a few tens of fs. Functionalization of the NHC ligands in $[Fe(btbip)_2]^{2+}$ (btbip = 2,6-bis(3-tert-butyl-imidazole-1-ylidene)pyridine) does not modify drastically the structural properties.[78] It is nearly impossible to interpret and rationalize the time-resolved experiments in this class of Fe(II) complexes merely on the basis of the energetics of the low-lying excited states within a static picture.

Papai et al[57b,57d,79] performed full quantum dynamics based on the spin-vibronic coupling model (linear and quadratic), involving 26 ($[Fe(bmip)_2]^{2+}$) and 36 ($[Fe(btbip)_2]^{2+}$) spin-orbit electronic states. Five degrees of freedom corresponding to three tuning modes (Fe-N/C stretching) that generate intrastate couplings $\boldsymbol{\kappa_i^{(n)}}$ and two coupling modes that induce the non-adiabatic couplings $\boldsymbol{\lambda_i^{(nm)}}$ were included in the simulations with the possibility of an additional time-dependent electric field for a linear polarized laser pump pulse.

This journal is © The Royal Society of Chemistry 20xx

Please do not adjust margins

Whereas this pioneering quantum dynamics simulations provide a detailed and clear picture of the ultrafast decay observed in these iron complexes within a few ps, namely an ultrafast ^{1}MLCT → ^{3}MLCT transition within 100 fs followed by a more or less slow decay to the ^{3}MC state due to the position of the MLCT/MC crossings, they do not enlighten the correlation between the electronic densities in play and the nuclear dynamics.

When examining the relative position of the MLCT and MC diabatic excited-state potentials as function of the nuclear displacements from Franck-Condon in different conditions (functionalized NHC, laser field, solvent)[57b,57d,79,80] we observe different responses of the MLCT and MC states to the tuning modes. These specific responses correlated with the electronic and nuclear flexibilities of coordination compounds are governed by the intrastate coupling $\boldsymbol{\kappa_i^{(n)}}$. Indeed, in NHC substituted complexes the tuning modes with large contribution of Fe-C bond stretching generate large $\boldsymbol{\kappa_i^{(n)}}$ in MC states and moderate values of different sign in MLCT states because of the nature of the Fe-carbene bonding.

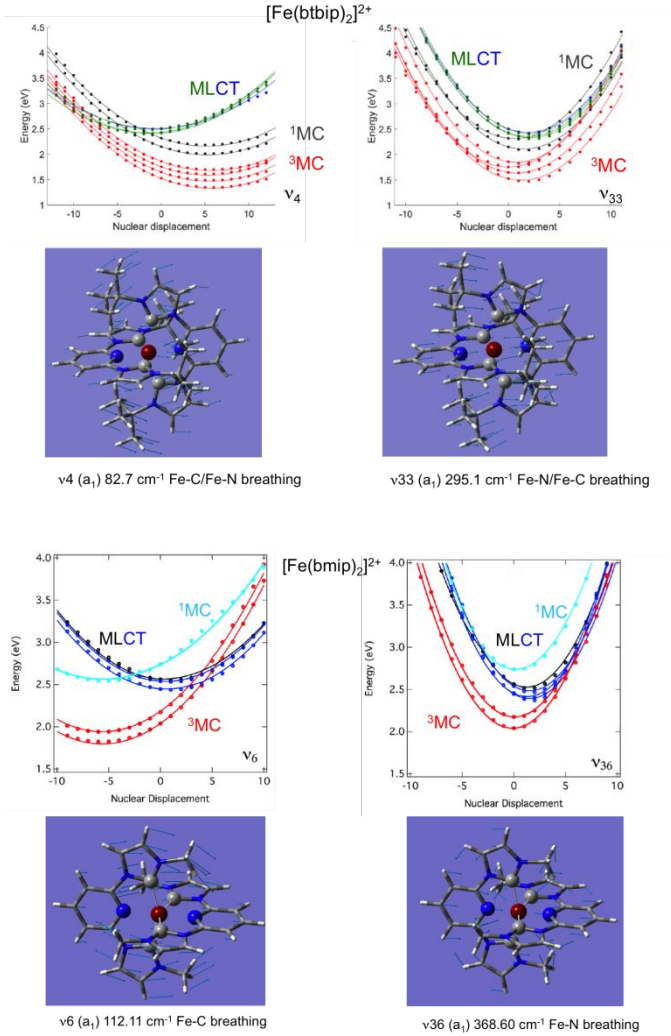

Figure 2. Cuts of the diabatic potential energy surfaces as function of the nuclear displacements associated to the dominant normal modes in $[Fe(bmip)_2]^{2+}$ (bottom) and $[Fe(btbip)^2]^{2+}$ (top). (Adapted from Ref. 57b and 79 with the permission of the American Chemical Society).

The consequence is an important shift in position and energy of the MC states from FC as compared to the MLCT states under early time nuclear vibrations generating conical intersections far away from Franck-Condon (Figure 2). When the Fe-N stretching dominates in the chosen tuning modes $\boldsymbol{\kappa_i^{(n)}}$ becomes negligible in MC states and is significant in MLCT states. Modifying the ligands, functionalizing them or adding solvent effects may affect the Fe-C/Fe-N stretching ratio in the tuning modes as well as the MC/MLCT electronic mixing and relative positions of the low-lying states.

This is illustrated by the different excited state dynamics observed in $[Fe(bmip)_2]^{2+}$ and $[Fe(btbip)_2]^{2+}$. In the bmip substituted complex Fe-C bond stretching mostly contributes to the a_1 breathing tuning mode ν6 generating large $\boldsymbol{\kappa_i^{(n)}}$ ($0.05 < \left\|\kappa_{\nu6}^{(MC)}\right\| < 0.09$ eV) for the two upper ^{1}MC states and four lowest ^{3}MC states and moderate intrastate couplings ($0.003 < \left\|\kappa_{\nu6}^{(MLCT)}\right\| < 0.01$ eV) in the two lowest ^{1}MLCT and three upper ^{3}MLCT states. In contrast the Fe-N bond stretching dominates the other a_1 tuning mode ν36 creating large $\boldsymbol{\kappa_i^{(n)}}$ ($0.05 < \left\|\kappa_{\nu36}^{(MLCT)}\right\| < 0.07$ eV) in the two lowest ^{1}MLCT and three upper ^{3}MLCT states and negligible intrastate couplings in the MC states ($\left\|\kappa_{\nu36}^{(MC)}\right\| < 0.005$ eV).[57b] Consequently the activation of ν6 will move drastically the ^{3}MC states ($\left\|\kappa_{\nu6}^{(MC)}\right\| \sim +0.09$ eV) in position and in energy with respect to the ^{1,3}MLCT states as illustrated by the cuts through the diabatic PES along ν6 (Figure 2). In the btbip-substituted complex the situation is more contrasted[79] with a similar activity of the a_1 tuning breathing ν4 mode that generates smaller intrastate couplings in the MC states ($\left\|\kappa_{\nu4}^{(MC)}\right\| \sim -0.06$ eV) than in $[Fe(bmip)_2]^{2+}$ and minor $\boldsymbol{\kappa_i^{(n)}}$ ($\left\|\kappa_{\nu4}^{(MLCT)}\right\| < +0.01$) of different signs in the MLCT states. More importantly an equal contribution of the Fe-C and Fe-N bond stretching's to the other a_1 tuning mode ν33 in $[Fe(btbip)_2]^{2+}$ with large values of $\boldsymbol{\kappa_i^{(n)}}$ of same signs ($\left\|\kappa_{\nu33}^{(MC,MLCT)}\right\| > 0.05$ eV) in both MC and MLCT states will prevent large shifts in position and energy of the MC potentials with respect to the MLCT potentials as observed in the bmip complex (Figure 2). Moreover, the sequence of MC/MLCT states is disrupted by the functionalization of the HNC ligand in $[Fe(btbip)_2]^{2+}$ as depicted in generating ^{1,3}MLCT/^{1}MC crossings near FC (Figure 2).

Within the first 100 fs the near-degeneracy of the ^{1}MLCT/^{3}MLCT states at FC and the limited nuclear motion makes the ^{1}MLCT → ^{3}MLCT transition efficient and ultrafast in both complexes. Then the dynamics beyond 200 fs is activated by the tuning modes. While ν6 induces a drastic shift of the ^{3}MC potentials generating ^{1,3}MLCT/^{3}MC conical intersections far away from FC in the bmip complex, ν4 generates ^{1,3}MLCT/^{1}MC crossings around FC in the btbip complex (Figure 2). When the second higher frequency tuning modes enter into play, the two molecules adopt different behaviors. In the case of $[Fe(bmip)_2]^{2+}$ ν36 creates large intrastate couplings in the ^{1,3}MLCT states generating ^{1,3}MLCT/^{3}MC crossings and dominates the population of the ^{3}MC states within a few hundred of fs. At longer time-scale the process is slowed down and part of the system gets trapped into the ^{3}MLCT state for 4 ps in agreement with the observed experimental time-scale of 9 ps. In $[Fe(btbip)_2]^{2+}$ the role of the second tuning mode ν_{33} is inhibited because it does act on the MC and MLCT potentials in the same way limiting the generation of accessible conical intersections (Figure 2). Instead coupling modes and SOC will activate efficient ^{1,3}MLCT →

^{1}MC transitions within 500 fs and population of the lowest ^{3}MC state within 2 ps.

When studying in details the theoretical results published on $[Fe(bpy)_3]^{2+}$[81]for which the spin-vibronic coupling model has never been applied we realize that we have here an ideal situation for ultrafast ^{1,3}MLCT → ^{5}MC decay (< 100 fs) as compared to the NHC substituted molecules discussed above. Indeed, only the Fe-N stretching and bending modes are in play. Consequently the early time vibrations less affect the MC states excluding opportunity for spawning conical intersections far away from FC as compared to NHC substituted systems. In contrast potentials associated to MLCT states may be slightly shifted in position and energy from FC supporting efficient ^{1,3}MLCT → ^{1}MC transition. Indeed, cuts of the calculated PES as function of Fe-N bond stretching and calculated absorption spectra of $[Fe(bpy)_3]^{2+}$ at different levels (*ab initio* and TD-DFT)[81] exhibit the presence of one ^{1}MC state in the vicinity of the ^{1,3}MLCT states in addition to ^{3}MC/^{5}MC crossings nearby FC (Figure 3). We may expect ultrafast and efficient SOC driven vibronic assisted ^{1}MLCT → ^{3}MLCT and ^{1,3}MLCT → ^{1,3}MC transitions within a few tens of fs and population of the ^{5}MC high-spin state as soon as the lowest ^{3}MC state is populated. Further quantum dynamics simulations based on wavepacket propagations are needed to confirm the mechanism and put in evidence the role of the ^{1}MC state.

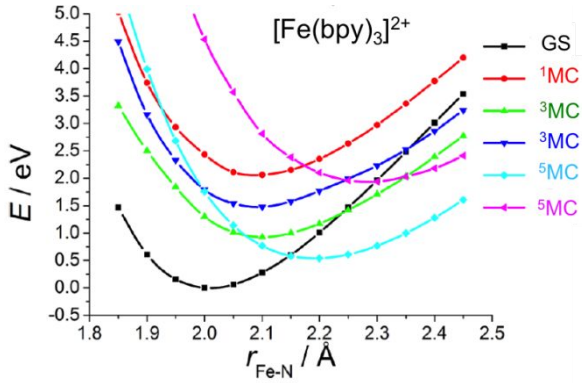

Figure 3. Cuts of the TD-DFT(B3LYP/TZP) calculated PES of $[Fe(bpy)_3]^{2+}$ as function of the Fe-N elongation (Adapted from Ref. 81a with the permission of the American Chemical Society).

The restricted number of normal modes included in the spin-vibronic Hamiltonian (up to five) and the accuracy of the electronic structure calculations are two limiting factors of fully quantum dynamics simulations that may bias the conclusions of the above studies dedicated to large transition metal complexes.

A recent work proposed by Zobel et al[69c] based on LVC model coupled with TSH dedicated to $[Fe(tpy)(pyz\text{-}NHC]^{2+}$ (tpy = 2,2' :6',2''-terpyridine ; pyz-NHC=1,1'-bis(2,6-diisopropylphenyl)pyrainyl-diimidazolium-2,2'-diylidene) illustrates the complexity of the analysis when increasing drastically the number of degrees of freedom in the simulation and the bias induced by reduced dimensionality. This study involving 20 singlet and 20 triplet electronic states, 244 normal modes, decoherence correction, SOC and solvent effects, while challenging, does not provide a sharp conclusion as far as the ultrafast dynamics is concerned in the absence of experimental data for this molecule. The manipulation of the LVC matrix by excluding some normal modes does not add clarity about the strong correlation between the electronic densities, tuning modes and intrastate couplings $\kappa_i^{(n)}$. The presence of one NHC ligand instead of two in $Fe(bmip)_2]^{2+}$ and $[Fe(btbip)_2]^{2+}$ let expect that the Fe-C stretching modes will have less influence on the early time dynamics despite the presence of three ^{3}MC states (2.56-2.76 eV) in the vicinity of the ^{1}MLCT absorbing states (2.62-2.88 eV).

The two-step kinetics of ultrafast photolysis from a heme—CO complex (Figure 4), namely τ < 50-70 fs attributed to the carbonyl loss and partial spin crossover and τ ~300-400 fs ascribed to spin transition to high-spin states[82] has been investigated in details by wavepacket quantum dynamics.[52]

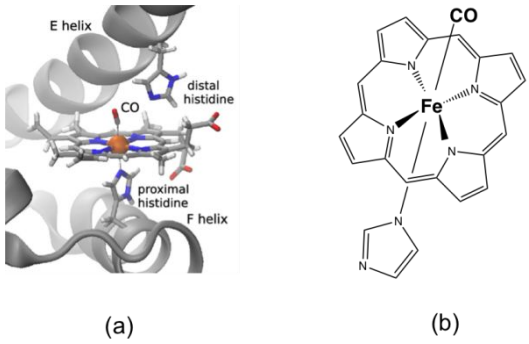

Figure 4. (a) Cartoon of the myoglobin active site (b) Schematic structure of the heme-CO model complex.

This complete quantum simulation includes 15 vibrational normal modes, the low-lying 18 singlet, 20 triplet and 20 quintet electronic states coupled by SOC and vibronically up to the fith order. The authors have concluded to an ultrafast CO release within 20 fs in the ^{1}MLCT band prior to singlet to triplet transition estimated at 75 fs and triplet to quintet transition at 450 fs within a sequential mechanism. When scrutinizing the correlation between electronic densities, active normal modes and intrastate couplings in the heme-CO model complex used in the theoretical study a more refined scenario can be proposed: after population of the Q band calculated at 2.73 eV, CO stretching (ν_{122} = 1478 cm^{-1}), in-plane N-stretching (ν_{23}=356 cm^{-1}) and to a lesser extend out-of-plane porphyrin motion (ν_{26} =376 cm^{-1}) (Figure 5) generate large intrastate couplings in some specific excited states close to the Q band.

This journal is © The Royal Society of Chemistry 20xx

Please do not adjust margins

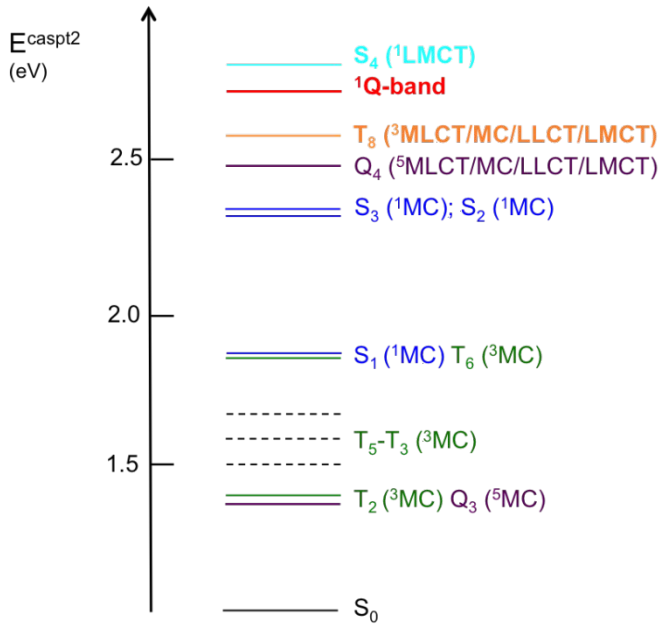

Scheme 2. CASPT2 calculated excited state diagram of the heme-CO model complex (Figure 4(b)).[52]

This leads to significant displacements of the potentials associated to the S_4 ^{1}LMCT state calculated at 2.83 eV ($\kappa_{122}^{(S4)}$=-0.50 eV, $\kappa_{23}^{(S4)}$ = -0.30 eV, $\kappa_{26}^{(S4)}$ = -0.15eV), to the T_8 triplet mixed MLCT/MC/LLCT/LMCT state calculated at 2.56 eV ($\kappa_{122}^{(T8)}$=-0.45, $\kappa_{23}^{(T8)}$ =-0.31, $\kappa_{26}^{(T8)}$=-0.20) and to the three lowest ^{1}MC states ($\left\|\kappa_{\nu 122}^{(^1MC)}\right\|$ >0.25) calculated between 1.90 eV and 2.36 eV.

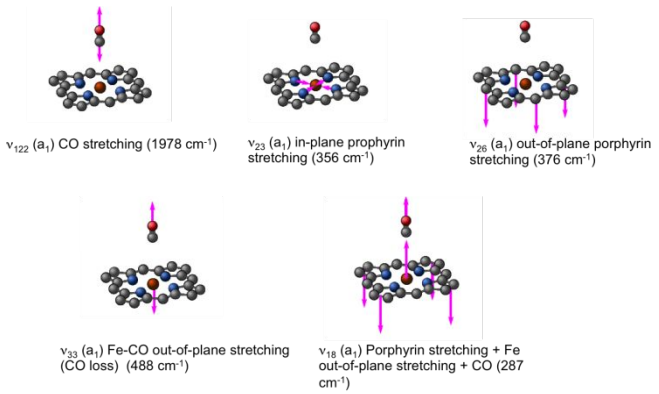

Figure 5. Major normal modes activated in the ultrafast CO photolysis in the heme-CO model complex (Figure 4 (b)) (Adapted from Ref. 52 with the permission of the authors).

Consequently a negative shift in position and energy of these electronic states with respect to the initially populated Q state induces a number of conical intersections favouring their efficient and ultrafast population in the first few tens of fs as illustrated by the diabatic population evolution shown in Figure 6.

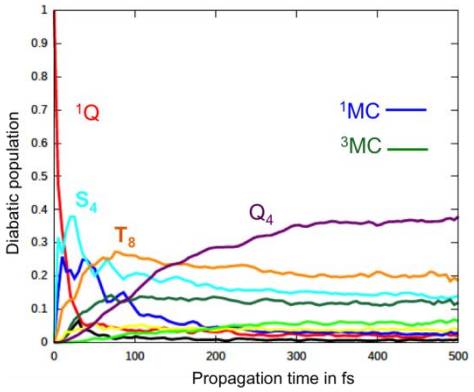

Figure 6. Time evolution of the diabatic population of the ^{1}Q, S_4, T_8, ^{1}MC and ^{3}MC excited states of the heme-CO model complex (Adapted from Ref. 52 including SI with the permission of the authors).

At the same time Fe-CO stretching ν_{33} (Figure 5) acts specifically on the pure ^{3}MC states that involve Fe-CO bonding/antibonding orbitals generating huge negative intrastate coupling ($\left\|\kappa_{\nu 33}^{(^3MC)}\right\|$ > 0.4 eV) leading to drastic shifts of the associated potentials along this coordinate that drives their efficient population within about 70 fs (Figure 6). These ^{3}MC states play certainly a key role in the ultrafast dissociation of CO observed in the first few tens of fs which cannot be solely attributed to the so-called ^{1}MLCT band as proposed previously.[52]

Interestingly the very close mode ν_{18} involving in addition to the Fe-out-of-plane CO dissociation the porphyrin ring motion (Figure 5) acts similarly to ν_{33} on the lowest ^{3}MC pure states but shifting the potentials in the opposite direction and less importantly. Moreover these two modes generate large intrastate couplings of opposite signs in the quintet states as well (Q_4: $\kappa_{33}^{(Q4)}$=-0.33, $\kappa_{18}^{(Q4)}$=+0.23). This certainly promotes triplet/quintet crossings that favour, together with SOC, efficient transition to the upper mixed MLCT/MC/LLCT/LMCT quintet state (Q_4 calculated at 2.48 eV) within 100-150 fs (Figure 6) and at longer time scales to the lowest ^{5}MC states.

Ruthenium(II) complexes. The de-correlation of ultrafast kinetics of intersystem crossing with heavy atom effects and SOC is one of the mysteries of molecular ultrafast photophysics in coordination chemistry. Whatever the metal center (from 1st-row to 3rd-row) and the ligands (presence of halides) the ultrafast kinetics (< 1 ps) appears to be insensitive to the chemical environment. An illustration is given by the ultrafast decay observed in $[Fe(bpy)_3]^{2+}$ and $[Ru(bpy)_3]^{2+}$, less than 50 fs for reaching the lowest high-spin state in both complexes.[74] The first non-adiabatic TSH dynamics study of $[Ru(bpy)_2]^{2+}$ including SOC on-the-fly has been proposed by Atkins et al.[67a] In contrast to previous investigation of the same complex[83] hops between singlet and triplet states are not estimated *a posteriori* but occur stochastically based on the change of electronic state populations. The lowest 14 singlet and 15 triplet states calculated on-the-fly at the TD-DFT level as well as the 177 normal modes were included in the simulation based on 101 random allowed trajectories within the energy range accessible by irradiation. The theoretical ^{1}MLCT $\rightarrow$ ^{3}MLCT time decay extracted

from the simulation τ^{ISC} ~ 26 fs agrees rather well with the experimental data. Moreover it is shown that ultrafast ISC does not depend solely of the high density of excited states in a limited domain of energy and large SOC. ISC is also promoted by vibronic effects as discussed previously for the Fe(II) complexes, the normal modes involving the metal center and the nitrogen atoms being particularly active in the process. Finally the population of the S_1 and T_1 states remains marginal within the first tens of fs excluding a Kasha's rule mechanism. In principle this gas phase study gives a realistic picture of the ultrafast ISC in $[Ru(bpy)_2]^{2+}$ but becomes prohibitive in term of cost for longer time scales.

One of the most famous metal based photoswitch is the nitrosyl complex $[RuCl(NO)(py)_4]^{2+}$ (py = pyridine) depicted in scheme 3.

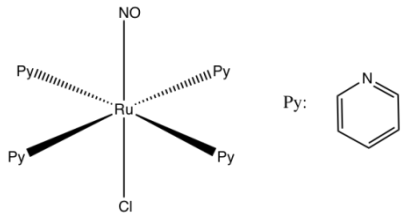

Scheme 3. Schematic structure of $[RuCl(NO)(py)_4]^{2+}$

Its reversible high photoswitching ability has motivated a number of experimental[84] and theoretical studies[85] in the past ten years. Whereas the mechanism of NO photoisomerization (Figure 7 (a) has been investigated by numerous static quantum chemical calculations, its nuclear dynamics has been recently studied for the first time.[67c] TSH including both non-adiabatic internal conversion and intersystem crossing has explored the early steps of the relaxation dynamics along different Ru-NO to Ru-ON pathways.

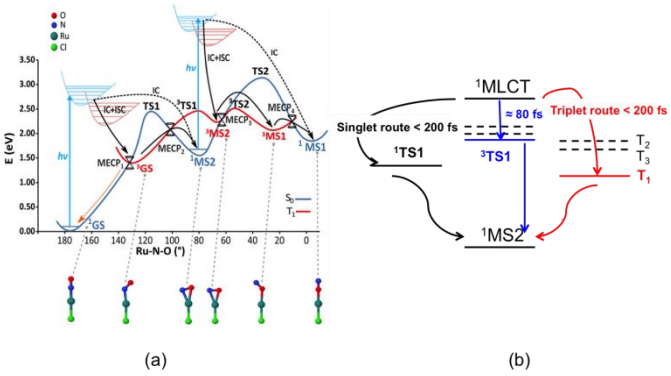

Figure 7. (a) Mechanism of $[RuCl(NO)(py)_4]^{2+}$ photoisomerization based on DFT(B3LYP) and MS-CASPT2 calculations (Adapted from Ref. 87 with the permission of the authors) (b) Three ultrafast decay pathways deduced from TSH dynamics.[67c]

The difficulties here are twofold: i) the electronic structure problem cannot be described consistently by density functional theory because the photoisomerization is a multiconfigurationanl problem; ii) trajectory instabilities due to near-degeneracy of the electronic states cause collapses or divergences. Fortunately, previous *ab initio* calculations of the mechanism based on multiconfigurational methods provided a gauge for the reliability of TD-DFT results, especially the position of state crossings, in this specific complex potential energy surface landscape.

On the basis of highly accurate stationary MS-CASPT2 calculations and non-adiabatic TSH dynamic simulations in gas phase three mechanisms were proposed to coexist with a 3:2:4 branching ratio within the first 200 fs (Figure 7 (b)). The metastable isomer MS2 is accessible via two routes upon ^{1}MLCT absorption at 473 nm, namely the triplet one combining fast ISC (~ 200 fs) and internal conversion and the singlet one following the lowest singlet PES via several conical intersections. A third pathway, not envisioned by static calculations and involving an ultrafast ISC (80 fs) has been put in evidence by the non-adiabatic dynamics. Interestingly the TSH non-adiabatic dynamics give a nice picture of the electronic densities evolution together with the Ru-N-O angle and Ru-NO bond length distribution as function of time.

The simulation of the complete photo-isomerization pathway, until the formation of the metastable isomer MS1 (Figure 7 (a)), is beyond the nowadays possibilities in terms of time-scale and trajectory stabilities. Whereas several approximations can be realistic for ultrafast photophysical processes they are hardly applicable to complex photochemical mechanisms involving transition metal complexes.

3.2 Excited state dynamics in Cu(I) complexes

Early time-resolved spectroscopic and femtosecond fluorescence up-conversion experiments[86] have shed a new light on the photophysics of Cu(I)- phenanthroline complexes studied for their redox and luminescent properties already in the 1980s[87] as competitor of $[Ru(bpy)_3]^{2+}$. $[Cu(dmp)_2]^+$ (dmp=2,9-dimethyl-1,10-phenanthroline) (Scheme 4) and related complexes represent one of the best case studies in the number of misleading interpretations of the photophysics of transition metal complexes on the basis of the restrictive two-state (S_1,T_1) spin-orbit coupled model.

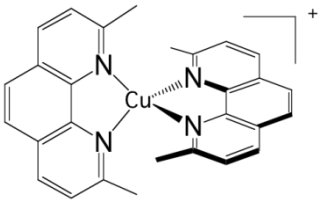

Scheme 4. Schematic structure of $[Cu(dmp)_2]^+$.

As already pointed out by Zgierski in 2003[88] and discussed more recently within the context of TADF[89] Cu(I) complexes are characterized by closely low-lying triplet states nearby S_1 and S_2 that may participate to the photophysics making the simple concept proposed for $[Ru(bpy)_3]^{2+}$ based on $S_1 \rightarrow T_1$ (MLCT) ultrafast ISC invalid. Moreover their excited state nuclear flexibility that makes their richness creates shallow minima and near-degeneracies on the low-lying PES calling for non-adiabatic quantum dynamics investigation based on accurate electronic structure data. By applying vibronic coupling Hamiltonian and wavepacket non-adiabatic dynamics to $[Cu(dmp)_2]^+$ within a fifteen "spin-orbit" states / eight normal modes model, including pseudo-Jahn-Teller (PJT) coordinate Capano et al[57c] clarified the mechanism of ultrafast decay in gas phase putting an end to a long-standing controversy. A fast $S_3 \rightarrow S_2$,S_1 internal conversion (~ 100 fs) occurs

This journal is © The Royal Society of Chemistry 20xx

Please do not adjust margins

nearby Franck-Condon together with the flattening of the ligands activated by pseudo-JT distortion within 400 fs. This distortion creates $S_1/T_2/T_3$ degeneracies favorable to efficient ISC within a sub-ps time-scale. The dominant normal modes are the symmetric Cu-N breathing ν_8 calculated at 99 cm^{-1} which activates the initial $S_3 \rightarrow S_2,S_1$ transition and the PJT rocking mode ν_{21} (b_3) that couples strongly S_1/S_2 and T_2/T_3.[57c]

The kinetics associated to the pseudo-JT distortion (400 fs) and consequently the efficient occurrence of ISC depends drastically of the environment.

A subsequent study combining TSH, wavepacket dynamics and QM/MM calculations[16c] argued to the little influence of the solvent on the initial ultrafast decay within the singlet excited states. However more recent studies dedicated to the early time structural dynamics of the lowest singlet states points to a nearly solvent independent fast component (~100 -200fs) and to a slow component arising from the solvent/molecular vibration interplay within ~1 ps.[90] A detailed study in gas phase by Du et al[91] put in evidence the role of the assisting motion of the methyl substituents at the early stage of the dynamics together with an interligand flattening stabilized at ~ 675 fs in agreement with the most recent experiments.

The long story of the Cu(I) complexes covering the last four decades clearly illustrates the necessity for an active and cooperative interplay between ultrafast time-resolved experiments and non-adiabatic dynamic simulations. This will be crucial to the success of potential applications in photovoltaic materials, OLED and TADF to name a few of them.

3.3 Ultrafast intersystem crossings in Re (I) complexes

Rhenium(I) complexes are among the most investigated 3rd-row transition metal complexes, both experimentally and theoretically. This growing interest over the last tow decades is due to their intriguing photophysical and photochemical properties able to generate specific functions in various environments, including large biological and macromolecular systems. These coordination compounds have been used as diagnostic and therapeutic tools, acting as luminescent and conformational probes[92] or in light-triggered electron transfer processes.[93] Rhenium(I) α-diimine carbonyls $[Re(L)(CO)_3(N,N)]^{n+}$ (L = halide, imidazole; N,N = bipyridine, phenanthroline) are thermally and photochemically robust and highly flexible synthetically. Structural variations of the N,N and L ligands has strong influence on the excited state properties of these chromophores. Visible light absorption opens the route to a wide range of applications such as sensors, probes, or emissive labels for bioimaging among others. One intriguing question raised by the first time-resolved luminescent experiments[94] is that the three energy domains and the three time domains put in evidence are relatively constant within this class of molecules whatever the choice of the ligands and the solvent. Indeed the 2D time-resolved luminescence spectra exhibit two luminescent signals at 500-550 nm and 550-600 nm associated to ultra-short time scales 80 fs < τ_1 < 150 fs and 0.3 ps < τ_2 < 1.5 ps, respectively and one signal below 610 nm with a phosphorescent time-scale varying from ns to ms, only τ_2 being slightly solvent dependent. The well accepted "cascade model" based on internal conversion (IC) vs. intersystem crossing (ISC) is unable to explain these experimental features. Early quantum dynamics simulations performed on this class of Re(I) complexes aimed at studying the role of structural dynamics on non-adiabatic ISC processes and at understanding why the "cascade model" breaks down.[95] This work together with the quantum dynamics studies performed on Fe(II) and Cu(I) complexes described in the previous section shed new insights onto the spin-vibronic mechanism of ISC establishing its importance in transition metal photophysics.[42]

Another stimulating question has been raised by halide substituted complexes $[Re(X)(CO)_3(bpy)]$ (X = Cl, Br, or I; bpy = 2,2'-bipyridine) which exhibit complex electronic structure and large spin−orbit effects that do not correlate with the heavy atom effects. Time-resolved luminescent experiments[94] performed on this class of complexes have pointed to the role of structural dynamics on the kinetics of ISC. The ^{1}MLCT→^{3}MLCT ISC kinetics in these 3rd-row compounds is slower than in $[Ru(bpy)_3]^{2+}$ or $[Fe(bpy)_3]^{2+}$. Moreover and counter intuitively, the expected heavy-atom effect within the series of halide-substituted complexes $[Re(CO)_3(bpy)]$ (X= Cl, Br, I) (Scheme 5), namely a decrease of the ISC rate along the Cl, Br and I sequence is not reproduced. Instead, the time scales of luminescent decays increase along the series with experimental values of τ_1 = 85 ± 8 (Cl), 128 ± 12 (Br) and 152 ± 8 (I) fs, τ_2 = 340 ± 50 (Cl), 470 ± 50 (Br) and 1180 ± 150 fs (I).[94a] Moreover, based on these experiments, a correlation has been proposed between the rhenium-halide stretch vibrational period and the kinetics of ISC (Figure 8).

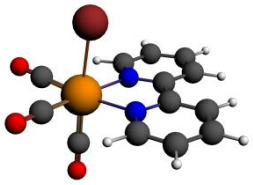

Scheme 5. Structure of the $[Re(X)(CO)_3(bpy)]$ complexes.

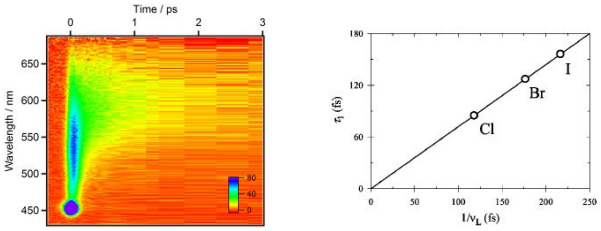

Figure 8. 2D time-resolved luminescence spectrum of $[Re(Cl)(CO)_3(bpy)]$ in CH_3CN (λ_{exc} = 400 nm) (a) and correlation of the ISC time-scales measured for $[Re(X)(CO)_3(bpy)]$ (X=Cl, Br, I) with the vibrational period of the Re-X stretching mode in similar complexes (Adapted from Ref. 94a with the permission of the American Chemical Society).

Static quantum chemical calculations based on TD-DFT calculations including solvent correction and SOC provide a clear qualitative picture of the photophysics of $[Re(X)(CO)_3(bpy)]$ controlled by the decay of two singlet (S_1-S_2) and three triplet (T_1-T_3) electronic excited states.[95b]

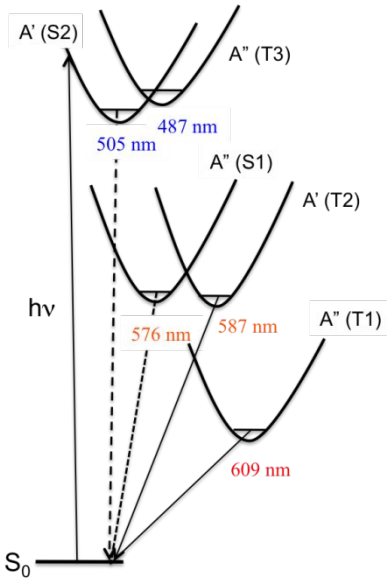

Scheme 6. Schematic representation of the potential energy curves associated to the low-lying excited states of [Re(Br)(CO)$_3$(bpy)].

The four lowest S_1, S_2, T_1 and T_2 photoactive electronic excited states of [Re(X)(CO)$_3$(bpy)] are characterized by a mixed MLCT/XLCT (halide-to-ligand-charge-transfer) character, the composition of which depends significantly of the nature of the halide. In agreement with Raman experiments[96] the XLCT character of the S_2/T_2 and S_1/T_1 excited states increase with the heavy atom effect. T_3 nearly degenerate with S_2 corresponds to an intra-ligand (IL) excited state localized on the bpy.

Pioneering non-adiabatic quantum dynamics performed on the bromide substituted complex [Re(Br)(CO)$_3$(bpy)][95a,95c] put in evidence the dominant normal modes able to activate significant vibronic couplings in this class of molecules. The normal modes activity is governed by symmetry rules (C_s symmetry in the present case), absolute values of the generated coupling terms $\kappa_i^{(n)}$ and $\lambda_i^{(nm)}$and by the character of the electronic excited state densities that correlate with the intrastate coupling term responsible for the shift in position and energy of the associated potential functions.[95c,95d] For instance, ν_9 and ν_{30} tuning modes associated to the CO vibrations (Figure 9) activate rather large intrastate couplings in the MLCT/XLCT states and act differently on S_1/T_1 and S_2/T_2 (symmetry rules) with $\kappa_9^{(S1,T1)} < 0$ and $\kappa_9^{(S2,T2)} > 0$ generating conical intersections favorable to an efficient population of these electronic states. The key vibrational modes are the CO motions because of the metal-carbonyl bonding characteristics and the bpy vibrations, which act on the IL excited state (T_3) and charge transfer electronic densities. The Re-X stretching mode ν_{11} acts similarly on S_1/T_1 and S_2/T_2 excited state electronic densities (Figure 9) with little impact on the potential shifts and generate rather small positive intrastate couplings in all states. The proposed correlation between the measured ISC time-scales and the Re-X vibration is fortuitous.

A revealing illustration of the correlation between the vibrational activity, the electronic densities and the intrastate couplings is given by a recent study extended to the whole series of complexes [Re(X)(CO)$_3$(bpy)] (X= F, Cl, Br, I).[97] The non-adiabatic dynamics of the complexes within 1.5 ps is performed in a multimode approach developed on diabatic functions associated to S_1, S_2, T_3, T_2 and T_1 giving rise to 11 "spin-orbit" electronic states and incorporate 14 normal modes (12 a' and 2 a") within the quadratic vibronic coupling (QVC) model. The multiplet components are treated explicitly and SOC as well as the intra- and inter-state electron-vibration coupling terms are introduced in the $W(Q)$ coupling matrix.

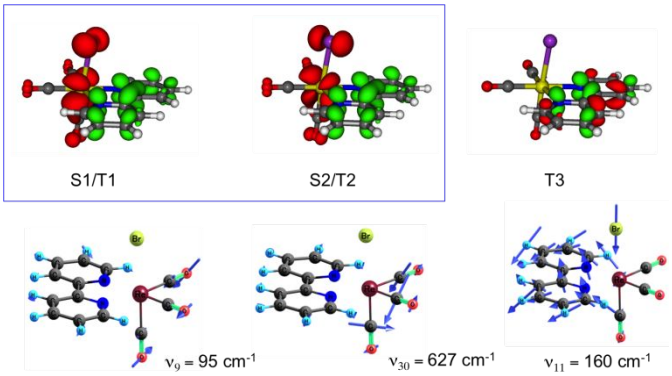

Figure 9. Differences in electronic densities accompanying the $S_0 \rightarrow S_1/T_1$, $S_0 \rightarrow S_2/T_2$ and $S_0 \rightarrow T_3$ transitions in [Re(Br)(CO)$_3$(bpy)] (top) and some associated dominant symmetric tuning modes responsible for the intrastate coupling $\kappa_i^{(n)}$.

The time evolution of the diabatic population of the absorbing S_2 excited state reveals an ultrafast exponential decay τ_1 within a few tens of fs common to the four investigated complexes (Figure 10). The early time theoretical decay of S_2/T_3 (in black in Figure 10) coincides nearly perfectly with the experimental τ_1 (in light blue in Figure 10) extracted from a 3-parameters global fit for X= Cl and Br.[94a] τ_1 is estimated at 93 ± 3 fs for X = Cl comparable to the experimental value of 85 ± 8 fs.[97]

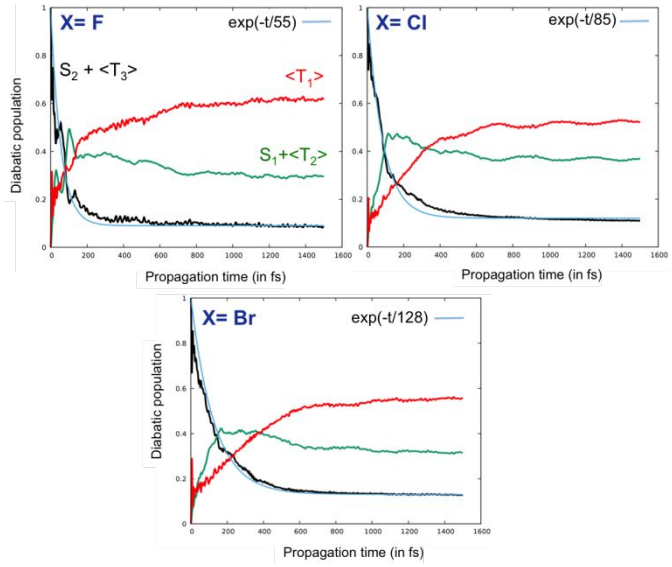

Figure 10. Time-evolution of the population of the low-lying T_3, S_2/T_2 and S_1/T_1 excited states in [Re(F)(CO)$_3$(bpy)] (a), [Re(Cl)(CO)$_3$(bpy)] (b) and [Re(Br)(CO)$_3$(bpy)] (c). For the sake of clarity the S_2/T_3 and S_1/T_2 populations are summed up. [97]

This journal is © The Royal Society of Chemistry 20xx

Please do not adjust margins

The simulations, including the one dedicated to the fluoride complex not investigated experimentally but predicted to decay within τ_1 = 55 fs, reproduce rather well the trends within the series, namely an increase of the time scales within the halide series from the lighter to the heavier atom. The vibronic couplings induced by the carbonyls and bipyridine vibrations drive this ultra-fast decay, which is accompanied by the population of the two intermediate states S_1 and T_2. The simulation performed on the iodide-substituted complex, not presented here, overestimates this effect with an over estimated τ_1 > 250 fs for an experimental value of ~150 fs. This could be explained by the approach in perturbation used to describe the SOC effects that may amplify artificially the XLCT character and underestimate $\kappa_i^{(n)}$ [illegible] in [Re(I)(CO)$_3$(bpy)]. The vibronic driven ultrafast decay of S_2 is followed by the decay of the intermediate states S_1 and T_2 within a few hundred of fs (τ_2) and induced essentially by SOC with T_1, the long-lived phosphorescent excited state. τ_2 is estimated at 367± 31 fs vs. an experimental value of 340 ± 50 fs in [Re(Cl)(CO)$_3$(bpy)].

The counterintuitive heavy atom effect pointed experimentally is well reproduced by the quantum dynamics. Indeed, when increasing the XLCT character of the S_1/T_1 and S_2/T_2 electronic states within the series (Table 1) the tuning modes associated to the carbonyl vibrations induce a decrease of the $\kappa_i^{(n)}$ intrastate couplings. As a consequence the perturbation of the diabatic potentials, namely shifts in position and in energy from the reference structure (Franck-Condon), diminishes as well as the probability of occurrences of critical geometries favorable to efficient transfer of population from S_2 to the intermediate states S_1 and T_2 and *in fine* to T_1.

Table 1. Intrastate coupling terms $\kappa_i^{(n)}$(in eV) induced in S_1, T_1, S_2,T_2 by the a' tuning mode associated to the CO vibrations calculated at ~ 95 cm^{-1} in [Re(X)(CO)$_3$(bpy)] (X = F, Cl, Br, I) and corresponding % of halide to bpy charge transfer character in these excited states along the series.[97]

X	F	Cl	Br	I
S_1	-0.0191	+0.0200	-0.0172	-0.0095
S_2	+0.0306	+0.0224	+0.0187	+0.0154
T_1	-0.0179	-0.0178	-0.0161	-0.0108
T_2	0.0364	0.0263	0.0190	0.0163
XLCT %*	7	17	28	56

* Within the limit of the electronic structure method (TD-DFT/B3LYP)

The mechanism of ultrafast ISC in [Re(X)(CO)$_3$(bpy)] is stimulated by vibronic coupling and controlled by the XLCT electronic density contributions within the first 100 fs, SOC being preeminent in the second step, namely the decay of the intermediate states and population of the long-lived T_1 state. Remarkably, this mechanism differs from the one discovered for the imidazole substituted complex [Re(imidazole)(CO)$_3$(phen)]$^+$ which posses pure MLCT states and an ^{3}IL (T_3) intermediate state efficiently populated within a few tens of fs. In this complex the equilibration between T_3 and T_1 occurs within 70-80 fs and is observed both experimentally and in the quantum dynamics simulation. T_3/T_1 vibronic coupling controlled the transfer of population to T_1. Interestingly when the normal modes associated to the phenanthroline vibrations are frozen in the simulation the $T_3 \rightarrow T_1$ transition is quenched. [95d,95e]

3.4 Other 3rd-row transition metal complexes

While excited state and photophysical properties of phosphorescent Ir(III) complexes have been extensively investigated because of their OLED potential their early time dynamics is less explored. Following experimental studies[98] dedicated to the ultrafast ISC in [Ir(ppy)$_3$] (ppy = 2-phenylpyridine), [Ir(ppy)$_2$(bpy)] (bpy : 2,2'-bipyridine) and [Ir(ppz)$_2$(dipy)] (ppz = 1-phenylpyrazole; dipy = 5-phenyldipyrrinato) Cui et al[99] studied the early time excited state non-adiabatic dynamics of the three complexes by means of TD-DFT based mixed *quantum-classical* Generalized-TSH (G-TSH) method including 5 singlet and 10 triplet electronic states coupled by SOC. The simulations reproduce rather well the experimental trends, namely an increase of ISC rate (65, 81 and 140 fs) along the [Ir(ppy)$_3$], [Ir(ppy)$_2$(bpy)], [Ir(ppz)$_2$(dipy)] series the electronic properties of the ligands modulating the ultrafast $S_n \rightarrow T_n$ decay via ISC and IC processes.

Combining their G-TSH method with QM/MM the same authors investigated the ultrafast excited state relaxation in [Os(bpy)$_3$] and [Os(bpy)$_2$(dpp)] (dpp=2,3-dipyridyl-pyrazine)[100] that exhibit rather significant inter-ligand-charge-transfer (ILCT) solvent dependence.[101]The simulations show that the ILCT plays a major role at the early time of the relaxation dynamics.

Finally, competition between the heavy atom effect and vibronic coupling in a series of donor-bridge-acceptor carbine metal-amide (metal = Cu, Ag, Au) emitter complexes has been scrutinized by means of non-adiabatic quantum dynamics including SOC. This study points to the competition between direct ultrafast ^{1}CT $\rightarrow$ ^{3}CT ISC (Au; < 100 fs) and via the population of an intermediate ^{3}IL state populated within ~ 65 fs in the Cu complex. This role of the intermediate state, largely stabilized when going from Au, to Ag and Cu becomes dominant in the Cu complex.[102]

Conclusion

The case studies presented in this perspective article illustrate with clarity why available quantum methods and current computational tools have to be used with care when dealing with ultrafast processes in transition metal complexes.

Whereas the static picture based on stationary electronic structure properties (eigenstates, eigenenergies, spin-orbit coupling) is correct for describing decays through "long –lived" S_1 and T_1 excited states following classical concepts developed in the 60's-70's for organic chromophores, this approach becomes inadequate for the interpretation of ultrafast relaxation processes within sub-ns in coordination chemistry unless chemical and experimental environments bring back "ideal" conditions. Indeed, the high density of states in a limited domain of energy, the variety of spin multiplicities, the nuclear flexibility, the degree of electronic mixing and the correlation between electronic densities and dominant normal modes generate crucial electron-vibration (vibronic) intrastate and inter-state couplings that control, together with SOC, the population in time of the individual excited states in the sub-ps regime. This opens the route to concurrent channels of deactivation hardly interpreted experimentally.

For further design of new coordination compounds with highly efficient functions applicable in various fields of chemistry and biology it is necessary either to control the photophysics chemically or environmentally for making the simple concepts pertinent or to

modify our way of thinking the complexity for a correct interpretation.

This complexity is even more dramatic when trying to properly include the environment effects within the context of relaxation dynamics, another active field of research.[103] The emergence of attoscience[104] able to follow electron molecular dynamics in complex systems[105] have opened a new domain dedicated to the correlated motion of electrons and nuclei in the attosecond (as) time scale[106] revealing a ground-breaking picture of molecular quantum properties with fundamental issues that remain to be discovered.

Conflicts of interest

There are no conflicts to declare.

References

[1] M. K. DeArmond, *Acc. Chem. Res.*, 1974, **7**, 309-315.

[2] K. W. Hipps, G. A. Merrell, G. A. Crosby, *J. Phys. Chem.*, 1976, **80**, 2232-2239; D. R. Striplin, G. A. Crosby, *Chem. Phys. Lett.*, 1994, **221**, 426-430; D. R. Striplin, G. A. Crosby, *J. Phys. Chem.*, 1995, **99**, 7977-7984; A. F. Rausch, M. E. Thompson, H. Yersin, *Inorg. Chem.*, 2009, **48**, 1928-1937; A.F. Rausch, M. E. Thompson, H. Yersin, *J. Phys. Chem. A* 2009, **113**, 5927-5932; A. Bossi, A. F. Rausch, M. J. Leitl, R. Czerwieniec, M. T. Whited, P. I. Djurovich, H. Yersin, M. E. Thompson, *Inorg. Chem.*, 2013, **52**, 12403-12415.

[3] J. Z. Zhao, S. M. Ji, W. H. Wu, W. T. Wu, H. M. Guo, J. F. Sun, H. Y. Sun, Y. F. Liu, Q. T. Li, L. Huang, *RSC Advances*, 2012, **2**, 1712-1728.

[4] J. Z. Zhao, K. J. Xu, W. B. Yang, Z. J. Wang, F. F. Zhong, *Chem. Soc. Reviews*, 2015, **44**, 8904-8939.

[5] B. K. T. Batagoda, P. I. Djurovich, S. Brase, M. E. Thompson, *Polyhedron*, 2016, **116**, 182-188; W. Wei, S. A. M. Lima, P. I. Djurovich, A. Bossi, M. T. Whited, M. E. Thompson, Polyhedron 2018, 140, 138-145.

[6] Y. Xu, J. Wang, W. Zhang, W. Li, W. Shen, *J. Photochem. Photobio. A: Chemistry*, 2017, **346**, 225-235.

[7] Photophysics of Organometallics Topics in Current Chemistry 29 Vol. Editor A. J. Lees 2010 Springer-Verlag Berlin-Heidelberg; G. Baryshnikov, B. Minaev, H. Agren, *Chem. Rev.*, 2017, **117**, 6500-6537.

[8] H. Yersin, J. Strasser, *Coord. Chem. Rev.* 2000, **208**, 331-364; H. Hofbeck, H. Yersin, *Inorg. Chem.*, 2010, **49**, 9290-9299; H. Yersin, A. F. Rausch, R. Czerwieniec, T. Hofbeck, T. Fischer, *Coord. Chem. Rev.*, 2011, **255**, 2622-2652; R. Czerwieniec, M. J. Leitl, H. H.H. Homeier, H Yersin, *Coord. Chem. Rev.*, 2016, **325**, 2-28.

[9] Photochemistry and Photophysics of Coordination Compounds *Top. in Curr. Chem.,* **280** Vol. Editors V. Balzani, S. Campagna 2007 Springer-Verlag Berlin-Heidelberg; Photophysics of Organometallics *Top. in Curr. Chem.,* **29** Vol. Editor A. J. Lees 2010 Springer-Verlag Berlin-Heidelberg; F. N. Castellano, Acc. Chem. Res. 2015, 48, 828-839; K. K. -W.Lo, *Acc. Chem. Res*., 2015, **48**, 2985-2995; K. Y. Zhang, Q. Yu, H. J. Wei, S. J. Liu, Q. Zhao, W. Huang, *Chem. Rev.*, 2018, **118**, 1770-18390.

[10] M. Chergui, *Acc. Chem. Res.* 2015, **48**, 801-808; A. Vlček Jr, *Coord. Chem. Rev.*, 2000, **200/202**, 933-977; M. Chergui, *Dalton Trans.*, 2012, **41**, 13022-13029.

[11] S. Straub, L. I. Domenianni, J. Lindner, P. Vöhringer, *J. Phys. Chem. B*, 2019, **123**, 7893−7904.

[12] H. Song, X. Wang, W. W. Yang, G. He, Z. Kuang, Y. Li, A. Xia, Y. -W. Zhong, F. Kong, *Chem. Phys. Lett.*, 2017, **683**, 322-328; A. M. Brown, C. E. McCusker, M. C. Carey, A. M. Blanco-Rodríguez, M. Towrie, I. P. Clark, A. Vlček, J. K. McCusker, *J Phys. Chem. A*, 2018, **122**, 7941−7953; M. C. Carey, S. L. Adelman, J. K. McCusker, *Chem. Sci.*, 2019, **10**, 134-144; I. V. Sazanovich, J. Best, P. A. Scattergood, M. Towrie, S. A. Tikhomirov, O. V. Bouganov, A. J. H. M. Meijer, J. A. Weinstein, *Phys. Chem. Chem. Phys.*,2014, **16**, 25775-25788; P. A. Scattergood, M. Delor, I. V. Sazanovich, O. V. Bouganov, S. A. Tikhomirov, A. S. Stasheuski, A. W. Parker, G. M. Greetham, M. Towrie, E. S. Davies, A. J. H. M. Meije, J. A. Weinstein, *Dalton Trans*, 2014, **43**,17677-17693; P. A. Scattergood, M. Delor, I. V. Sazanovich, M. Towrie, J. A. Weinstein, *Faraday Discuss.*, 2015, **185**, 69-86.

[13] P. Kim, M. S. Kelley, A. Chakraborty, N. L. Wong, R. P. Van Duyne, G. C. Schatz, F. N. Castellano, L. X. Chen*, J. Phys. Chem. C*, 2018, **122**, 14195−14204.

[14] K. Kunnus, M. Vacher, T. C.B. Harlang, K. S. Kjær, K. Haldrup, E. Biasin, T. B. van Driel, M. Pápai, P. Chabera , Y. Liu, H. Tatsuno,C. Timm, E. Källman, M. Delcey, R. W. Hartsock, M. E. Reinhard, S. Koroidov, M. G. Laursen, F. B. Hansen, P. Vester , M. Christensen, L. Sandberg, Z. Németh, D. S. Szemes, E. Bajnóczi, R. Alonso-Mori, J. M. Glownia, S. Nelson, M. Sikorski, D. Sokaras, H. T. Lemke, S. E. Canton, K. B. Møller , M. M. Nielsen, G. Vankó, K. Wärnmark, V. Sundström, P. Persson, M. Lundberg , J. Uhlig, K. J. Gaffney, *Nature Commun.*, 2020, **11**, 634-644.

[15] M. Iwamura, K. Kimoto, K. Nozaki, H. Kuramochi, S. Takeuchi, T. Tahara, *J. Phys. Chem. Lett.*, 2018, **9**, 7085−7089.

This journal is © The Royal Society of Chemistry 20xx

Please do not adjust margins

[16] (a) M. Iwamura, H. Watanabe, K. Ishii, S. Takeuchi, T. Tahara, *J. Am. Chem. Soc.*, 2011, **133**, 7728–7736; (b) L. Hua, M. Iwamura, S. Takeuchi, T. Tahara, *Phys. Chem. Chem. Phys.*, 2015, **17**, 2067-2077; (c) G. Capano, T. J. Penfold, M. Chergui, I. Tavernelli, *Phys. Chem. Chem. Phys.*, 2017, **19**, 19590-19600; (d) L. Shen, T. -F. He, L.-Y. Zou, J. -F. Guo, A. -M. Ren, *Organic Electronics*, 2020, **81**, 105664-1056674; (e) G. Levi, E. Biasin, A. O. Dohn, H. Jonsson, *Phys. Chem. Chem. Phys.*, 2020, **22**, 748-757.

[17] M. Delor, P. A. Scattergood, I. V. Sazanovich, A. W. Parker, G. M. Greetham, A. J. H. M. Meijer M. Towrie, J. A. Weinstein, *Science*, 2014, **346**, 1492-1494; M. Delor, T. Keane, P. A. Scattergood1, I. V. Sazanovich, G. M. Greetham, M. Towrie, A. J. H. M. Meijer, J. A. Weinstein, *Nature Chem.*, 2015, **7**, 689-695; M. Delor1, S. A. Archer, T. Kean, A. J. H. M. Meijer1, I; V. Sazanovich, G. M. Greetham, M. Towrie, J. A. Weinstein, *Nature Chem.*, 2017, **9**, 1099-1104.

[18] M.A.L. Marques; C.A. Ullrich; F. Nogueira; A. Rubio; K. Burke; E.K.U. Gross, eds. (2006) Time-Dependent Density Functional Theory. Springer-Verlag. *ISBN 978-3-540-35422-2*; M. E. Casida, Theoretical and Computational Chemistry, Vol. 4, Elsevier: New York, 1996; pp. 391–439; M. E. Casida, C. Jamorski, K. C. Casida, D. R. Salahub, *J. Chem. Phys.*, 1998, **108**, 4439; R. E. Stratmann, G. E. Scuseria, M. J. Frisch, *J. Chem. Phys.*, 1998, **109**, 8218; Hirata, M. Head-Gordon, *Chem. Phys. Lett.*, 1999, **302**, 375.

[19] Sherrill, C. David; Schaefer III, Henry F. (1999). Löwdin, Per-Olov (ed.). The Configuration Interaction Method: Advances in Highly Correlated Approaches. *Advances in Quantum Chemistry*. **34**. San Diego: Academic Press. pp. 143–269.

[20] Roos B.O. (1992) The Multiconfigurational (MC) Self-Consistent Field (SCF) Theory. In: Roos B.O. (eds) *Lecture Notes in Quantum Chemistry*. Lecture Notes in Chemistry, vol **58**. Springer, Berlin, Heidelberg.

[21] B. O. Roos, P. R. Taylor, P. E. M. Siegbahn, *Chem. Phys.*, 1980, **48**, 157-173.

[22] K. Andersson, P. –Å. Malmqvist, B.O. Roos, A. Sadlej, K. Wolinski. *J. Phys. Chem.*, 1990, 94, 5483-5486; K. Andersson, P. –Å. Malmqvist, B.O. Roos, *J. Chem. Phys.*, 1992, **96**, 1218-1226.

[23] M. Turki, C. Daniel, S. Záliš, A. Vlček, J. van Slageren, D. J. Stufkens, *J. Am. Chem. Soc.*, 2001, **123**(46), 11431-11440.

[24] M. Fumanal, C. Daniel, *J. Comp. Chem.*, 2016, **37**, 2454-2466.

[25] J. Olsen, B. O. Roos, P. Jörgensen, H. J. A. Jensen, *J. Chem. Phys.*, 1988, **89**, 2185 – 2192.

[26] D. Ma, G. Li Manni, L. Gagliardi, *J. Chem. Phys.*, 2011, **135**, 044128.

[27] G. Li Manni, F. Aquilante, L. Gagliardi, *J. Chem. Phys.*, 2011, **134**, 034114.

[28] M. R. Hermes, L. Gagliardi, *J. Chem. Theory Comput.*, 2019, **15**, 972 – 986 ; R. Pandharkar, M. R. Hermes, C. J. Cramer, L. Gagliardi, *J. Phys. Chem. Lett.*, 2019, **10**, 5507 – 5513.

[29] J. Ivanic, *J. Chem. Phys.*, 2003, **119**, 9364 – 9376.

[30] R. Pandharkar, M. R. Hermes, C. J. Cramer, L. Gagliardi, *J. Phys. Chem. Lett.*, 2019, **10**, 5507 – 5513.

[31] M. Joani, M. S. Gordon, *Phys. Chem. Chem. Phys.*, 2018, **20**, 2615-2626; M. Joani, M. S. Gordon, *J. Phys. Chem. A.*, 2019, **123**, 1260-1272; M. Joani, M. S. Gordon, *Phys. Chem. Chem. Phys.*, 2020, **22**, 1475-1484.

[32] K. H. Marti, M. Reiher, *Phys. Chem. Chem. Phys.*, 2011, **13**, 6750 – 6759; S. Sharma, G. K.-L. Chan, *J. Chem. Phys.*, 2012, **136**, 124121.

[33] C. J. Stein, M. Reiher, *J. Chem. Theory Comput.*, 2016, **12**, 1760 – 1771; C. J. Stein, M. Reiher, *J. Comput. Chem.*, 2019, **40**, 2216 – 2226.

[34] Q. M. Phung, S. Wouters, K. Pierloot, *J. Chem. Theor. Comput.*, 2016, **12**, 4352-4361; Q. M. Phung, K. Pierloot, *J. Chem. Theor. Comput.*, 2019, **15**, 3033-3043; M. A. Reiher, *Chimia*, 2009, **63**, 140-145.

[35] Mardirossian, N.; Head-Gordon, M. *Mol. Phys.*, 2017, **115**, 2315-2372.

[36] C. Daniel, Density Functional Theories and Coordination Chemistry, Reference Module in Chemistry, Molecular Sciences and Chemical Engineering, Elsevier, 2020, ISBN 9780124095472, https://doi.org/10.1016/B978-0-12-409547-2.14828-0)

[37] L. Gagliardi, D. G. Truhlar, G. Li Manni, R. K. Carlson, C. E. Hoyer, J. W. L. Bao, *Acc. Chem. Res.*, 2017, **50**, 66-73.

[38] A. Heil, M. Kleinschmidt, C. M. Marian, J. Chem. Phys. 2018, 149, 64106; C. M. Marian, A. Heil, M. Kleinschmidt, *Wires's Comput. Mol. Science*, 2019, **9**, E1394.

[39] Ferré, N.; Filatov, M.; Huix Rotllant, M. (eds) 2016, Density Functional Theory for Excited States, *Topics in Current Chemistry*, vol. **368**, Springer, Berlin ; C. Daniel, Density Functional Theories and Coordination Chemistry, Reference Module in Chemistry, Molecular Sciences and Chemical Engineering, Elsevier, 2020, ISBN 9780124095472, https://doi.org/10.1016/B978-0-12-409547-2.14828-0).

[40] C. Daniel, *Coord. Chem. Rev.* **2015**, *282-283*, 19-32 ; S. Xu, J. E. T. Smith, S. Gozem, A. I. Krylov, J. M. Weber, *Inorg. Chem.*, 2017, **56**, 7029-7037 ; K. Falahati, C. Hamerla, M. Huix-Rotllant, I. Burghardt, *Phys. Chem. Chem. Phys.*, 2018, **20**, 12483-12492.

[41] H.Köppel,W. Domcke, and L. S. Cederbaum, *Adv. Chem. Phys.*, 1984, **57**, 59–246.

[42] T. J. Penfold, E. Gindensperger, C. Daniel, C. M. Marian, *Chem.*

Rev., 2018, **118**, 6975-7625.

[43] D. C. Ashley, E. Jakubikova, *Coord. Chem. Rev.*, 2017, **337**, 97-111; C. Daniel, in Density Functional Methods for Excited States *Book series: Topics in Current Chemistry*, Vol. 2016, **368**, 377-413; N. M. S. Almeida, R. G. McKinlay, M. J. Paterson (2014) Computation of Excited States of Transition Metal Complexes. In: Macgregor S., Eisenstein O. (eds) *Computational Studies in Organometallic Chemistry*; *Structure and Bonding*, vol **167**. Springer, Cham.

[44] L. Lang, F. Neese, *J. Chem. Phys.*, 2019, **150**, 10414; F. Neese, *J. Am. Chem. Soc.*, 2006, **128**, 10213-10222; F. Neese, T. Petrenko, D. Ganyushin, G. Olbrich, *Coord. Chem. Rev.*, 2007, **251**, 288-327 ; C. Duboc, D. Ganyushin, K. Sivalingam, KM. –N.Collomb, F. Neese, *J. Phys. Chem. A.,* 2010, **114**, 10750-10758.

[45] E. van Lenthe, A.E. Ehlers, E.J. Baerends, *J. Chem. Physics*, 1999, **110**, 8943.

[46] B. de Souza, F Giliandro, F. Neese, R. Izsák, *J. Chem. Theory Comput.*, 2019, **15**, 1896−1904.

[47] P.-Å. Malmqvist, B.O. Roos, B. Schimmelpfennig, *Chem. Phys. Letters*, 2002, **357**:230-240.

[48] B.A. Heß, C.M. Marian, U. Wahlgren, O. Gropen. *Chem. Phys. Lett.*, 1996, **251**:365-371.

[49] C. M. Marian, *Wire's Comput. Mol. Sci.*, 2012, **2**, 187-203.

[50] F. Plasser, M. Ruckenbauer , S. mai, M. Oppel, P. marquetand, L. Gonzalez, *J. Chem. Theory Comput*., 2016, **12**, 1207-1219.

[51] M. Fumanal, F. Plasser, S. Mai, C. Daniel, E. Gindensperger, *J. Chem. Phys*., 2018, **148**, 124119.

[52] K. Falahati, H. Tamura, I. Burghardt, M. Huix-Rotlant, *Nature Commun*., 2018, **9**:4502.

[53] N. Balakrishnan, C. Kalyanaraman, N. Sathymurthy, *Phys. Rep*., 1997, **280**, 79-144; G. G. Balint-Kurti, R. N. Dixon, C. C. Marston, *Int. Rev. Phys. Chem*., 1992, **11**:2, 317-344; H. –D. Meyer, F. Gatti, G. A. Worth, Multidimensional Quantum Dynamics, Wiley-VCH, Weinheim, 2009).

[54] H. Beck, A. Jäckle, G. A. Worth, H.-D. Meyer, *Phys. Rep*., 2000, **324**:1,1.

[55] U. Manthe, *J. Chem. Phys.*, 2008, **128**, 164116.

[56] M. Fumanal, E. Gindensperger, C. Daniel, *J. Chem. Theory Comput*., 2017, **13**, 1293-1306; M. Fumanal, E. Gindensper, C. Daniel, *Phys. Chem. Chem. Phys.*, 2018, **20**, 1134-1141; Y. Harabuchi, J. Eng, E. Gindensperger, T. Taketsugu, S. Maeda, C. Daniel, *J. Chem. Theory Comput.*, 2016, **12**, 2335-2345; J. Eng, C. Gourlaouen, E. Gindensperger, C. Daniel, *Acc. Chem. Res*., 2015, **48**, 809-817.

[57] (a) M. Fumanal, E. Gindensperger, C. Daniel, *J. Phys. Chem. Lett.*, 2018, **9**, 5189-5195; (b) M.Pápai, G. Vankó, T. Rozgonyi, T. J. Penfold, *J. Phys. Chem. Lett.*, 2016, **7**, 2009-2014; (c) G. Capano, M. Chergui, U. Rothlisberger, I. Tavernelli, T. J. Penfold, *J. Phys. Chem. A*, 2014, **118**, 9861-9869 ; (d) M.Pápai,T. Rozgonyi, T. J. Penfold, M. N. Nielsen, K. B.Moller, *J. Chem. Phys.*, 2019, **151**, 104307.

[58] I. Burghardt, H. –D. Meyer, L. S. Cederbaum, *J. Chem. Phys*., 1999, **111**, 2927-2939.

[59] **G**. A. Worth, M. Robb, I. Burghardt, *Faraday Discuss.*, 2004, **127**, 307-323; B. Lasorne, G. A. Worth, M. A. Robb, *WIREs Comput. Mol. Sci.*, 2011, **1**, 460-475.

[60] G. Richings, I. Polyak, K. Spinlove, G. Worth, I. Burghardt, B. Lasorne, *Int. Rev. Phys. Chem.*, 2015, **34**, 269-308.

[61] D. V. Shalashilin, *J. Chem. Phys.*, 2009, **130**, 244101.

[62] M. Ben-Nun, J. Quenneville, T. J. Martinez, *J. Phys. Chem. A*, 2000, **104**, 5161-5175.

[63] D. V. Makhov, W. J. Glower, T. J. Martinez, D. V. Shalashilin, *J. Chem. Phys.*, 2014, **141**, 054110.

[64] A. Bera, J. Ghosh, A. Bhattacharya, *J. Chem. Phys.*, 2017, **147**, 044308.

[65] J. C. Tully, *Chem. Phys.*, 1990, **93**, 1061-1071.

[66] S. Mai, P. Marquetand, L. GonzaLez, *WIREs Comput. Mol Sci.*, 2018, **8**:e1370.

[67] (a) A. J. Atkins, L. Gonzalez, *J. Phys. Chem. Lett.*, 2017, **8**, 3840-3845; (b) S. Mai, L. Gonzalez, *Chem. Sci.*, 2019, **10**, 10405-10411 ; (c) F. Talotta, M. Boggio-Pasqua, L. Gonzalez, *Chem. Eur. J*., 2020, **26**, 11522-11528 ; (d) S. Mai, M. F. S. J. Menger, M. Marazzi, D. L. Stolba, A. Monari, L. Gonzalez, *Theor. Chem. Acc.*, 2020, **139** :65.

[68] F. Plasser, S. Gomez, M. F. S.J. Menger, S. mai, L. Gonzalez, *Phys. Chem. Chem. Phys.*, 2019, **21**, 57-69.

[69] (a) F. Plasser, S. Mai, M. Fumanal, E. Gindensperger, C. Daniel, L. Gonzalez, *J. Chem. Theory Comput*., 2019, **15**, 5031-5045; (b) S. Mai, L. Gonzalez, *J. Chem. Phys*., 2019, **151**,244115-1-14 ; (c) J. P. Zobel, O. S. Bokareva, P. Zimmer, C. Wölper, M. Bauer, L. Gonzalez, *Inorg. Chem.* : https://dx.doi.org/10.1021/acs.inorgchem.0c02147)

[70] S. K. Min, F. Agostini, E. K. U. Gross, *Phys. Rev. Lett.*, 2015, **115**, 073001; F. Agostini, S. K. Min, A. Abedi, E. K. U. Gross, *J. Chem. Theory, Comput*., 2016, **12**, 2127-2143; J. -K. Ha, I. S. Lee, S. K. Min, *J. Phys. Chem. Lett*., 2018, **9**, 1097-1104.

[71] S. K. Min, F. Agostini, I. Tavernelli, E. K. .U. Gross, *J. Phys. Chem. Lett.*, 2017, **8**, 3048-3055.

[72] F. Agostini, B. F. E. Curchod, *WIREs, Comput. Mol. Sci*., 2019, **9**, E1417.

[73] S. Decurtins, P. Guthlich, C. Kohler, H. Spiering, A. Hauser, *Chem. Phys. Lett*., 1984, **105**, 1-4; A. Hauser, A. Vef, P. Adler, *J. Chem.*

This journal is © The Royal Society of Chemistry 20xx

Please do not adjust margins

Phys., 1991, *95*, 8710.

[74] O. Bräm, F. Messina, A. M. El-Zohry, A. Cannizzo, M. Chergui, *Chem. Phys.*, 2012, **393**, 51-57; A. Cannizzo, F. van Mourik, W. Gawelda, G. Zgrablic, C. Bressler, M. Chergui, *Angew. Chem*., 2006, **118**, 3246-3248; N. H. Damrauer, G. Cerullo, A. Yeh, T. R. Boussie, C. V. Shank, J. K. McCusker, *Science*, 1997, **275**, 54-57; A. T. Yeh, C. V. Shank, J. K. McCusker, *Science*, 2000, **289**, 935-938; A. Cannizzo, C. J. Milne, C. Consani, W. Gawelda, Ch. Bressler, F. van Mourik, M. Chergui, *Coord. Chem. Rev.*, 2010, **254**, 2677-2686; W. Zhang et al Nature, 2014, 509, 345-348; G. AuBöck, M. Chergui, 2015, *Nature*, **7**, 629-633.

[75] Y. Liu, T. C. Harlang, S. E. Canton, P. Chabera, K. Suarez-Alcantara, A. Fleckhaus, D. A. Vithanage, E. Göransson, A. Corani, R. Lomoth, V. Sundström, K. Wärnmark, *Chem. Commun*., 2013, **57**, 6412-6414.

[76] P. Chabera, K. S. Kjaer, O. Prakash, A. Honarfar, Y. Liu, L. A. Fredin, T. C. Harlang, S. Lidin, J. Uhlig, V. Sundström, R. Lomoth, P. Persson, K. Wärnmark, *J. Phys. Chem. Lett.,* 2018, **9**, 459-463; K. S. Kjaer et al, *Science*, 2019, **363**, 249-253.

[77]L. A. Fredin, M. Papai, E. Rozsalyi, G. Vanko, K. Wärnmark, V. Sundström, P. Persson, *J. Phys. Chem. Lett.*, 2014, **5**, 2066-2071.

[78] M. Papai, T. J. Penfold, K. B. moller, *J. Phys. Chem. C*, 2016, **120**, 17234-17241.

[79] M. Papai, M. Simmermacher, T. J. Penfold, K. B. Moller, *J. Chem. Theory Comput*., 2018, **14**, 3967-3974.

[80] M. Papai, M. Abedi, G. Levi, E. Biasin, M. M.Nielsen, K. B. Moller, *J. Phys. Chem. C*, 2019, **123**, 2056-2065.

[81] (a) M. Papai, G. Vanko, C. de Graaf, T. Rozgonyi *J. Chem. Theory Comput.* 2013, **9**, 509-519; (b) C. Sousa, C. de Graaf, A. Rudavskyi, R. Broer, J. Tatchen, M. Etinski, C. M. Marian*, Chem. A Eur. J*., 2013, **19**, 17541-17551.

[82] M. Levantino, , G. Schiro, , H. T. Lemke, G. Cottone, *Laser Nat. Commun*., 2015, **6**, 6772; M. Levantino et al, *Struct. Dynam*. 2015, **2**, 041713; S. Franzen, L. Kiger, C. Poyart, J. L. Martin, *Biophys. J*., 2001, 80, 2372-2385.

[83] I. Tavernelli, B. F. E. Curchod, U. Rothlisberger, *Chem. Phys.*, 2011, **391**, 101-109.

[84] D. Schaniel, B. Cormary, I. Malfant, V. Lydie, V. Theo, V. Bernard, K. V. Kramer, H. –U. Gudel, *Phys. Chem. Chem. Phys*., 2007, **9**, 3717-3724; B. Cormary, I. malfant, L. Valade, M. Buron-Le-Cointe, L. Toupet, T. Todorova, B. Delley, D. Schaniel, N. Mockus, T. Voike, K. Fejfarova, V. Petricek, M. Dusek, *Acta Crystallogr. Sect. B* 2009, **65**, 787; B. Cormary, S. Ladeira, K. Jacob, P. G. Lacroix, T. Voike, D. Schaniel, I. Malfant, *Inorg. Chem.*, 2012, **51**, 7492-7501; A. G. De Candia, J. P. Marcolongo, R. Etchenique, L. D. Slep, *Inorg. Chem.*, 2010, **49**, 6925-6930.

[85] J. Sanz Garcia, F. Alary, M. Boggio-Pasqua, I. M. Dixon, I. Malfant, J. –L. Heully, *Inorg. Chem.*, 2015, **54**, 8310-8318; J. Sanz Garcia, F. Alary, M. Boggio-Pasqua, I. M. Dixon, J. –L. Heully, *J. Mol. Model.*, 2016, **22**, 284; F. Talotta, J. –L. Heully, F. Alary, I. M. Dixon, L. Gonzalez, M. Boggio-Pasqua, *J. Chem. Theory, Comput*., 2017, **13**, 6120-6130.

[86] L. X. Chen, G. Shaw, I. Novozhilova, T. Liu, G. Jennings, K. Attenkofer, G. Meyer, P. Coppens, *J. Am. Chem. Soc*., 2003, 125, 7022-7034; M. Iwamura, S. Takeuchi, T. Tahara, *J. Am. Chem. Soc.*, 2007, **129**, 5248-5256; G. B. Shaw, C. D. Grant, H. Shirota, E. W. Castner, G. J. Meyer, L. X. Chen, *J. Am. Chem. Soc*., 2007, **129**, 2147-2160.

[87] M. W. Blaskie, D. R. McMillin, *Inorg. Chem*., 1980, **19**, 3519-3522; C. O. Dietrich-Buchecker, P. A. Marnot, J. -P. Sauvage, J. R. Kirchhoff, D. R. McMillin, *J. Chem. Soc. Chem. Commun*., 1983, 513-515; D. G. Cuttel, S. –M. Kuang, P. E. Fanwick, D. R. McMillin, R. A. Walton, *J. Am. Chem. Soc*., 2002, **124**, 1,6-7; N. Armaroli, G. Accorsi, F. Cardinali, A. Listorti, *Top. Curr. Chem.,* 2007, **280**: 69-115 Springer-Verlag Berlin Heidelberg.

[88] M. Zgierski*, J. Chem. Phys*., 2003, **118**, 4045.

[89] A. Stoianov, C. Gourlaouen, S. Vela, C. Daniel, *J. Phys. Chem. A*, 2018, **122**, 1413-1421.

[90] G. Levi, E. Biasin, A. O. Dohn, H. Jonsson, *Phys. Chem. Chem. Phys*., 2020, **22**, 748-757.

[91] L. Du, Z. Lan, *Phys. Chem. Chem. Phys*., 2016, **18**, 7641-7650.

[92] K. K. W. Lo, *Acc. Chem. Res*., 2020, **53**, 32-44; E. B. Bauer, A.A Haase, R. M. Reich, D. C. Crans, F. E. Kühn, *Coord. Chem. Rev*., 2019, **393**, 79-117; L. K. McKenzie, H. E. Bryant, J. A. Weinstein, *Coord. Chem. Rev*., 2019, **379**, 2-29; A. M. –H. Yip, K.K W. Lo, *Coord. Chem. Rev*., 2018, **361**, 138-163; L. C. C. Lee, K. –K. Leung, K. K. W. Lo, *Dalton Trans.*, 2017, **46**, 16357-16380.

[93] J. J. Warren, M. E. Ener, A. Vlcek Jr, J. R. Winkler, H. B. Gray, *Coord. Chem. Rev*., 2012, **256**, 2478-2487; C. Shih, A. K. Museth, M. ABrahamsson, A. M. Blanco-Rodriguez, A. J. Di Bilio, J. Sudhamsu, B. B. Crane, K. L. Ronayne, M. Towrie, A. Vlcek Jr., J. H. Richards, J. R. Winkle, H. B. Gray, *Science*, 2008, **320**, 1760-1762; A. M. Blanco-Rodriguez, M. Busby, C. Gradinaru, B. R. Crane, A. J. Di Bilio, P. Matousek, M. Towrie, B. S. Leigh, J. H. Richards, A. Vlcek, Jr., H. B. Gray, *J. Am; Chem. Soc*., 2006, **128**, 4365-4370; A. J. Di Bilio, B. R. Crane, W. A. Wehbi, C. N. Kiser, M. M. Abu-Omar, R. M. Carlos, J. H. Richards, J. R. Winkler, H. B. Gray, *J. Am. Chem. Soc*., 2001, **123**, 3181-3182.

[94] (a) A. Cannizzo, A. M. Blanco-Rodriguez, A. El Nahhas, J. Sebera, S. Zalis, A. Vlcek, Jr., M. Chergui, *J. Am. Chem. Soc.*, 2008, **130**, 8967-8974; (b) A. El Nahhas, C. Consani, A. M. Blanco-Rodriguez, K. M. Lancaster, O. Braem, A. Cannizzo, M. Towrie, I. P. Clark, S. Zalis, M.

Chergui, A. Vlcek Jr, *Inorg. Chem*., 2011, **50**, 2932-2943.

[95] (a) J. Eng, C. Gourlaouen, E. Gindensperger, C. Daniel, *Acc. Chem. Res.*, 2015, **48**, 809-817; (b) C. Gourlaouen, J. Eng, M. Otsuka, E. Gindensperger, C. Daniel, *J. Chem. Theory Comput*., 2015, **11**, 99-110; (c) Y. Harabuchi, J. Eng, E. Gindensperger, T. Taketsugu, S. Maeda, C. Daniel, *J. Chem. Theory Comput*., 2016, **12**, 2335-2345; (d) M. Fumanal, E. Gindenspeger, C. Daniel, *J. Chem. Theory Comput*., 2017, **13**, 1293-1306; (e) M. Fumanal, E. Gindensper, C. Daniel, *Phys. Chem. Chem. Phys.*, 2018, **20**, 1134-1141

[96] B. D. Rossenaar, D. J. Stufkens, A. Vlcek Jr., *Inorg. Chem*., 1996, **35**, 2902-2909.

[97] J. Eng, C. Daniel, E. Gindenspeger, in preparation (2020).

[98] K. C. tang, K. L. Liu, I. C. Chen, *Chem. Phys. Lett*., 2004, **386**, 437-441; S. -H. Wu, J. -W. Ling, S. –H. Lai, M. –J. Huang, C. –H. Chen, I. C. Chen, *J. Phys. Chem. A*, 2010, **114**, 10339-10344; E. Pomarico, M. Silatani, F. Messina, O. Bräm, A. Cannizzo, E. Barranoff, J. –H. Klein, C. lambert, M. Chergui, M. Dual, *J. Phys. Chem. C*., 2016, **120**, 16459-16469.

[99] X. –Y. Liu, Y. –H. Zhang, W. –H. Fang, G. Cui, *J. Phys. Chem. A*, 2018, **122**, 5518-5532.

[100] Y. –G. Fang, L. –Y. Peng, X. –Y. Liu, W. –H. Fang, G. Cui, *Comput. Theor. Chem*., 2019, **1155**, 90-100.

[101] J. L. Pogge, D. F. Kelley, *Chem. Phys. Lett.*, 1995, **238**, 16-24; J. P. Cushing, C. Butoi, D. F. Kelley, *J. Phys. Chem. A,* 1997, **101**, 7222-7230; O. Bräm, F. Messina, E. Barranoff, A. Cannizzo, M. K.Nazeeruddin, M. Chergui, *J. Phys. Chem. C*, 2013, **117**, 15958-15966.

[102] J. Eng, S. Thompson, H. Goodwin, D. Credgington, T. J. Penfold, *Phys. Chem. Chem. Phys.***,** 2020, **22**, 4659-4667.

[103] T. R. Nelson, A. J. White, J. A. Bjorgaard, A. E. Sifain, Y. Zhang, B. Nebgen, S. Fernandez-Alberti, D. Moyrsky, A. E. Roitberg, S. Tretiak, *Chem. Rev*., 2020, **120**, 2215-2287; J. Norell, M. Odelius, M. Vacher, *Structural Dynamics-US*, 2020, **7**, 024101; Weingart O., *Curr. Organ. Chem*., 2017, **21**, 586-601.

[104] P. M. Paul, E. S. Toma, P. Breger, G. Mullot, F. Auge, P. Balcou, H. G. Muller, P. Agostini, *Science*, 2001, **292**, 1689-1692; M. Hentschel, R. Kienberger, Ch. Spielmann, G. A. Reider, N. Milosevic, T. Brabec, P. Corkum, U. Heinzmann, M. Drescher, F. Kausz, *Nature*, 2001, **414**, 509-513.

[105] F. Calegari, D. Ayuso, A. Trabattoni, L. Belshaw, S. De Camillis, S. Anumula, F. Frassetto, L. Poletto, A. Palacios, P. Decleva, J. B. Greenwood, F. martin, M. Nisoli, *Science*, 2014, **346**, 336-339.

[106] M. Nisoli, P. Decleva, F. Calegari, A. Palacios, F. Martin, *Chem. Rev*., 2017, **117**, 10760; A. Palacios, F. Martin, *WIREs Comput. Mol. Sci.*, 2020, e1430.

This journal is © The Royal Society of Chemistry 20xx

Please do not adjust margins

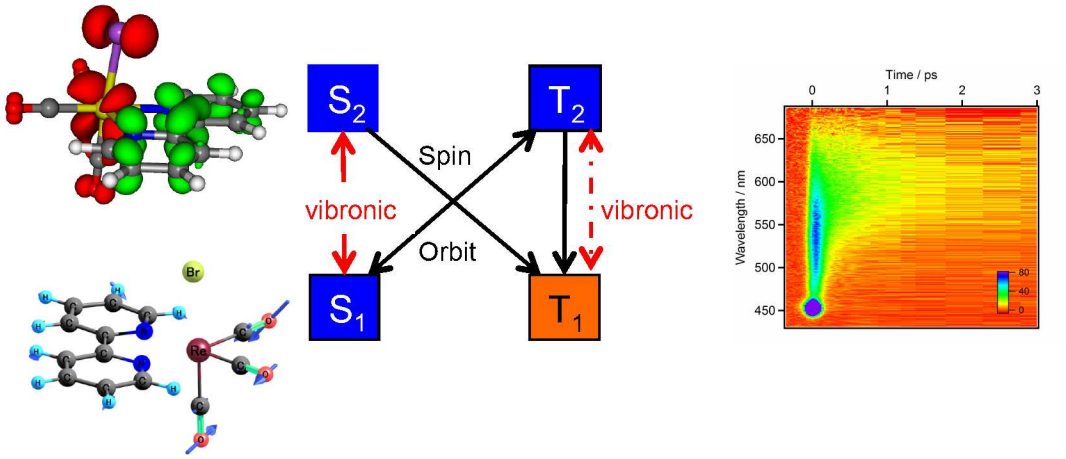

Correlation between electronic densities and active molecular vibrations drives spin-vibronic mechanism of ultrafast decays in coordination chemistry

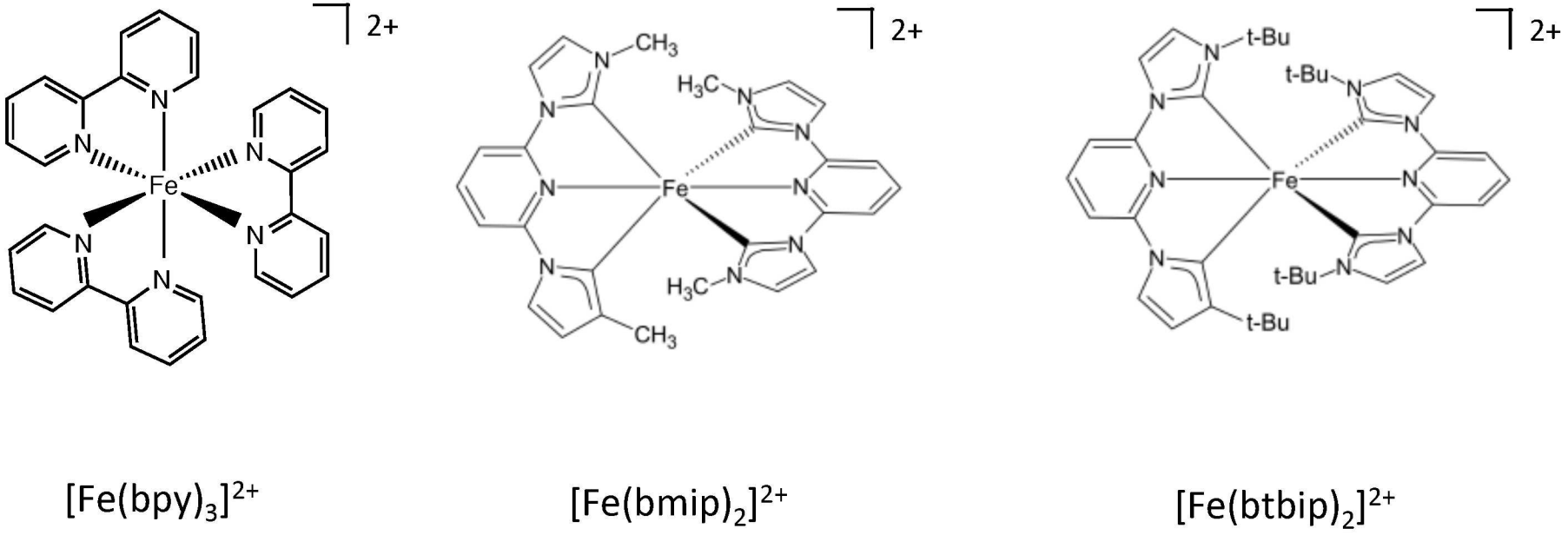

$[Fe(bpy)_3]^{2+}$ $[Fe(bmip)_2]^{2+}$ $[Fe(btbip)_2]^{2+}$

Figure 1. Schematic structures of $[Fe(bpy)_3]^{2+}$, $[Fe(bmip)_2]^{2+}$ and $[Fe(btbip)_2]^{2+}$ complexes.

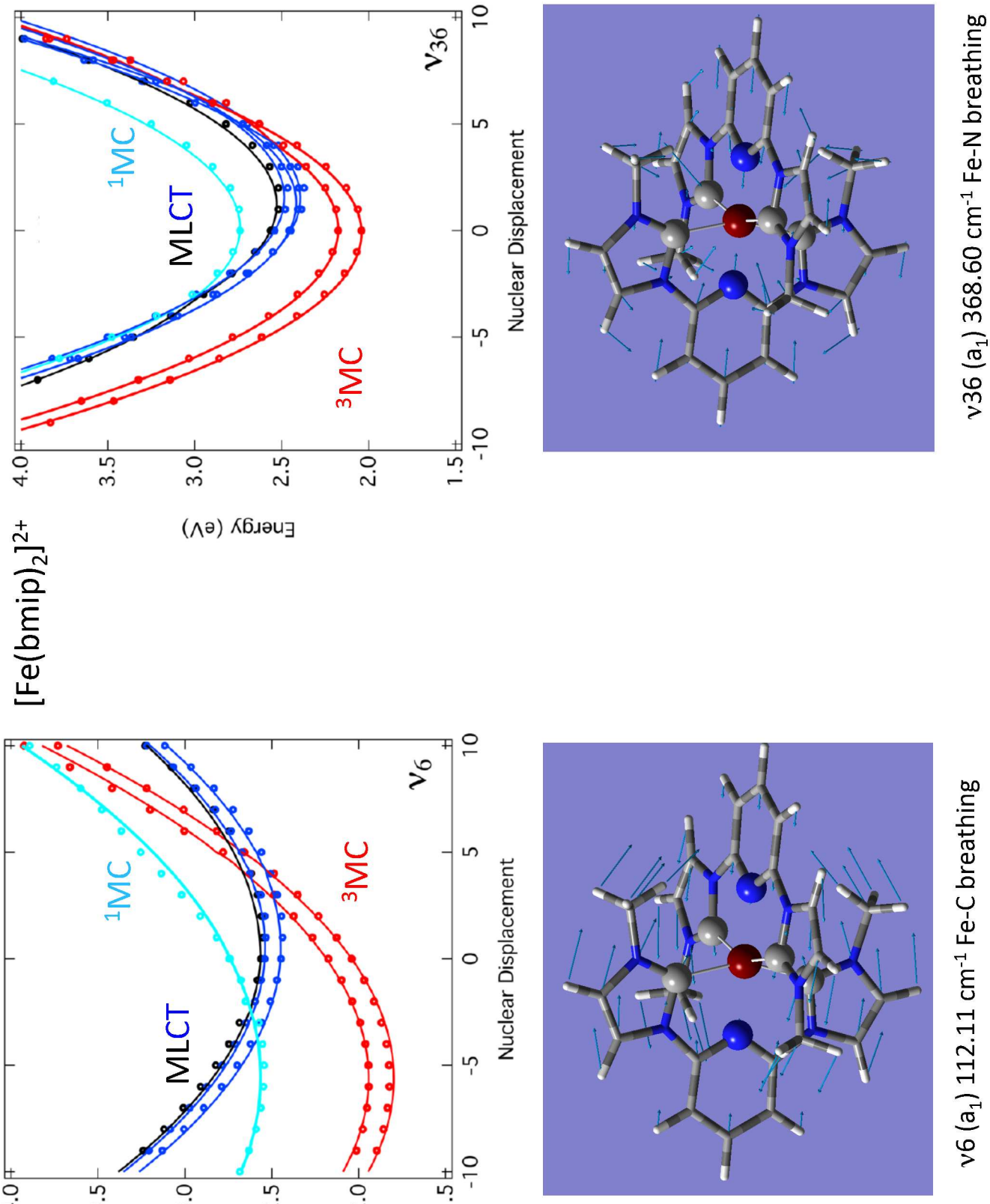

Figure 2 bottom

Figure 2 top

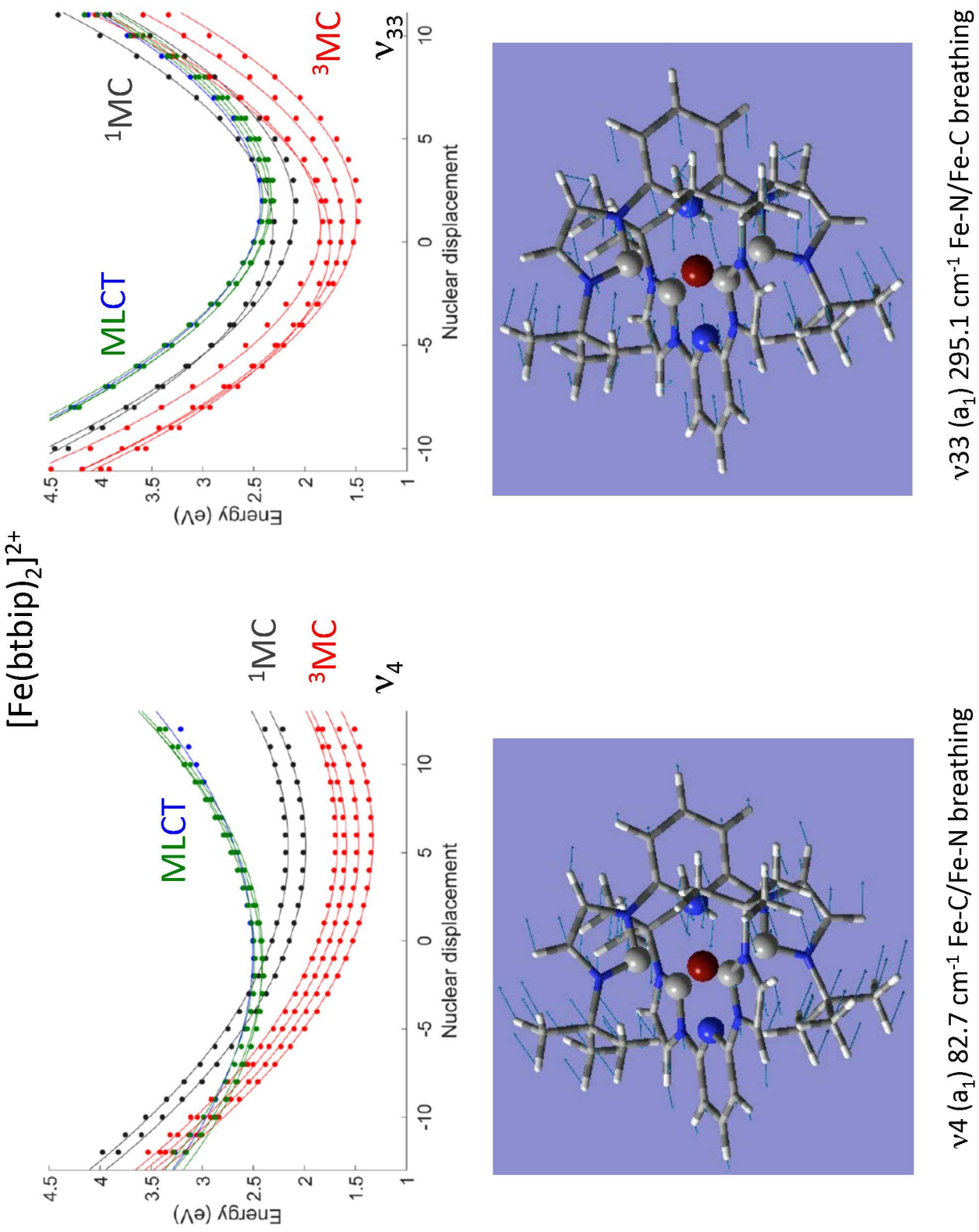
[Fe(btbip)2]2+
MLCT
1MC
3MC
ν4
ν33
Energy (eV)
Nuclear displacement
ν4 (a1) 82.7 cm-1 Fe-C/Fe-N breathing
ν33 (a1) 295.1 cm-1 Fe-N/Fe-C breathing

Figure 2. Cuts of the diabatic potential energy surfaces as function of the nuclear displacements associated to the dominant normal modes in $[Fe(bmip)_2]^{2+}$ (bottom) and $[Fe(btbip)^2]^{2+}$ (top). (Adapted from Ref. 57b and 79 with the permission of the American Chemical Society).

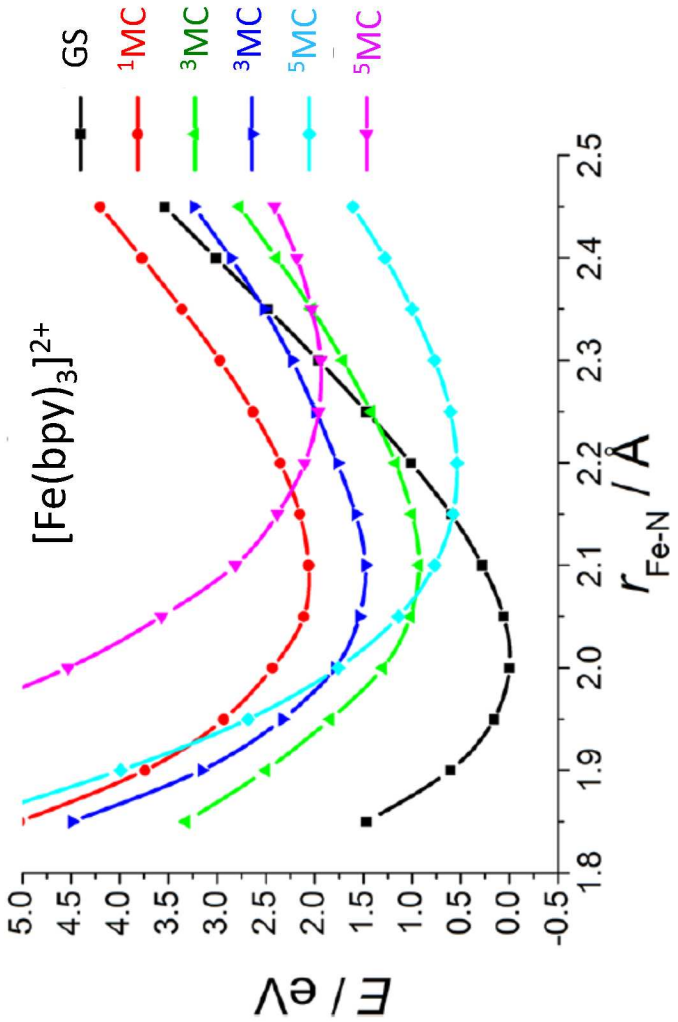

Figure 3. Cuts of the TD-DFT(B3LYP/TZP) calculated PES of $[Fe(bpy)_3]^{2+}$ as function of the Fe-N elongation (Adapted from Ref. 81a with the permission of the American Chemical Society).

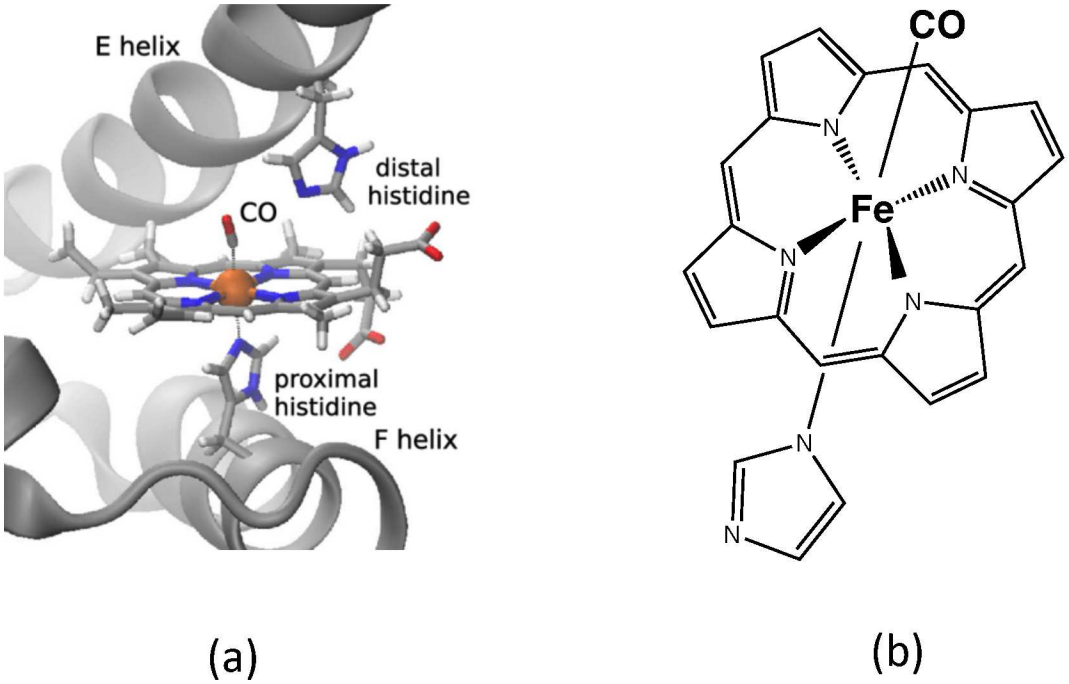

Figure 4. (a) Cartoon of the myoglobin active site (b) Schematic structure of the heme-CO model complex.

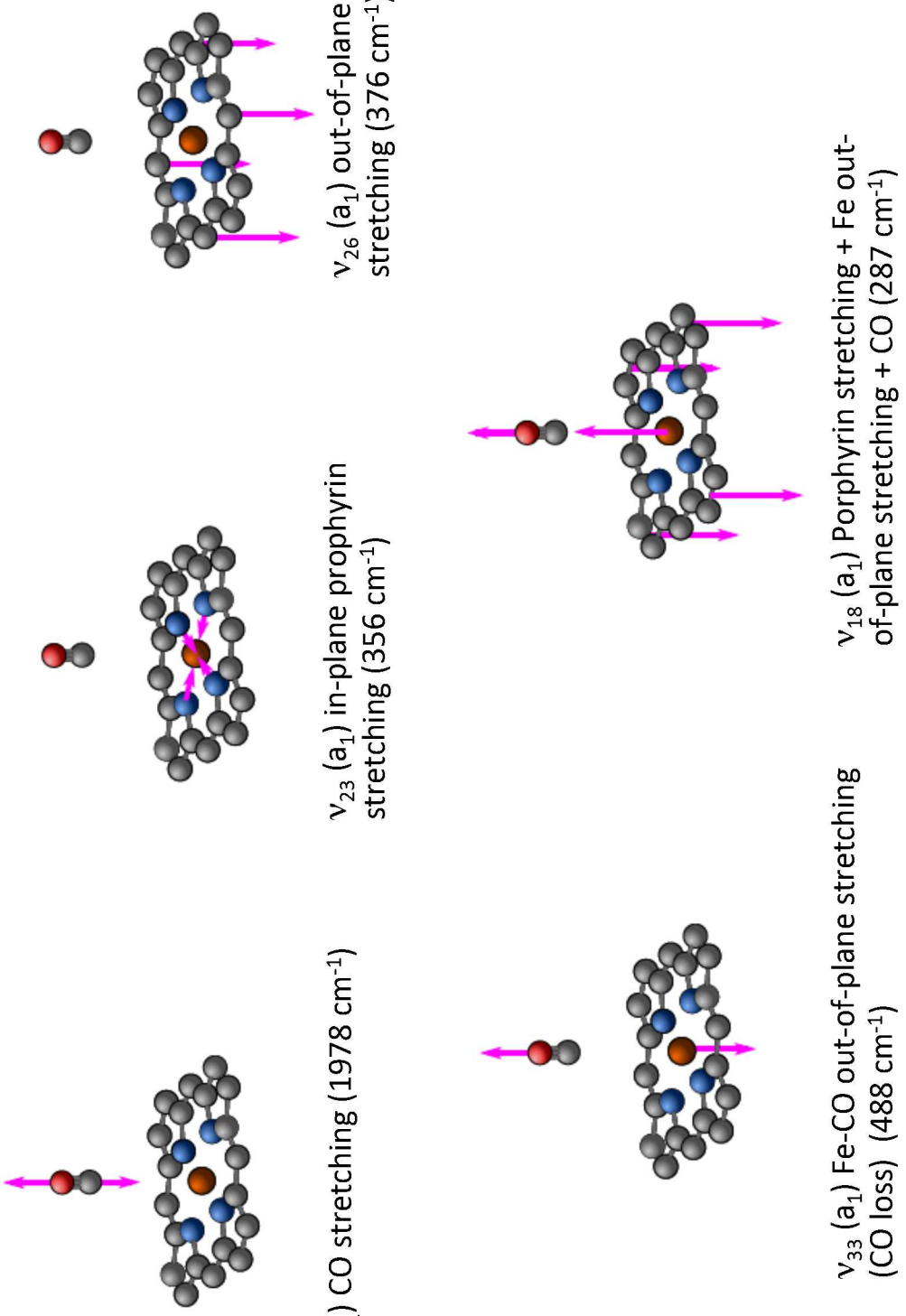

Figure 5. Major normal modes activated in the ultrafast CO photolysis in the heme-CO model complex (Figure 4 (b)) (Adapted from Ref. 52 with the permission of the authors).

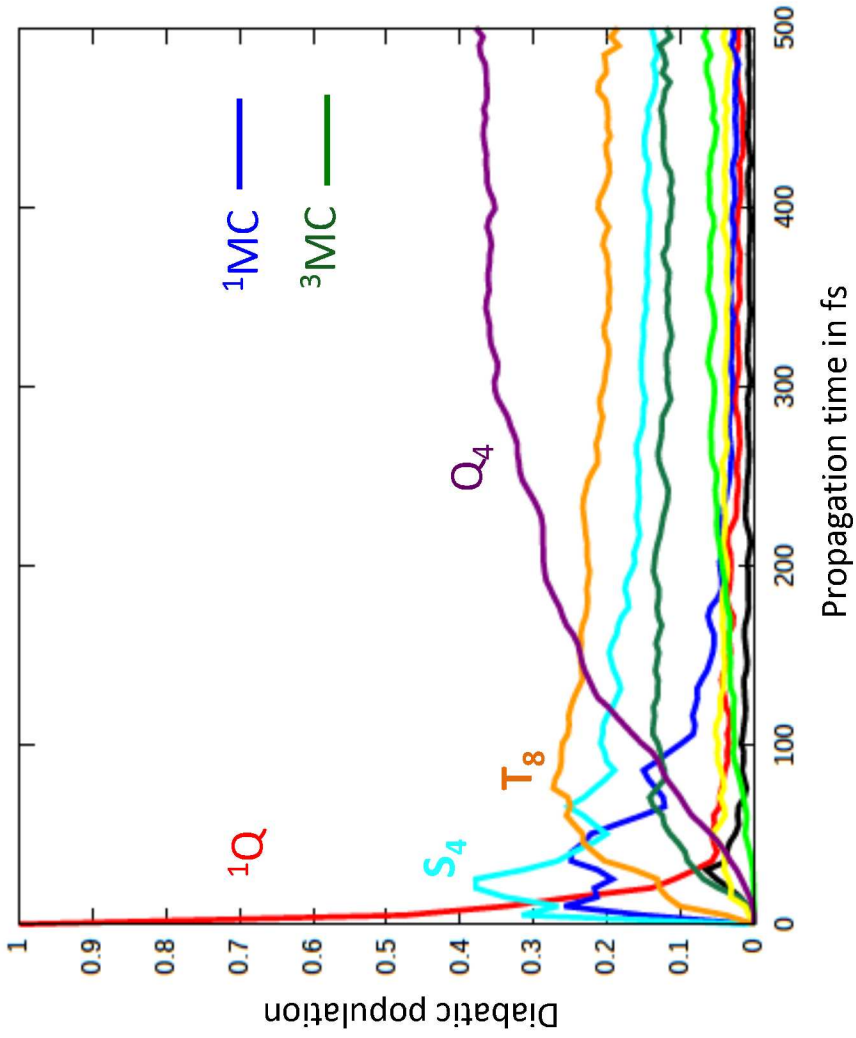

Figure 6. Time evolution of the diabatic population of the ^{1}Q, S_4, T_8, ^{1}MC and ^{3}MC excited states of the heme-CO model complex (Adapted from Ref. 52 including SI with the permission of the authors).

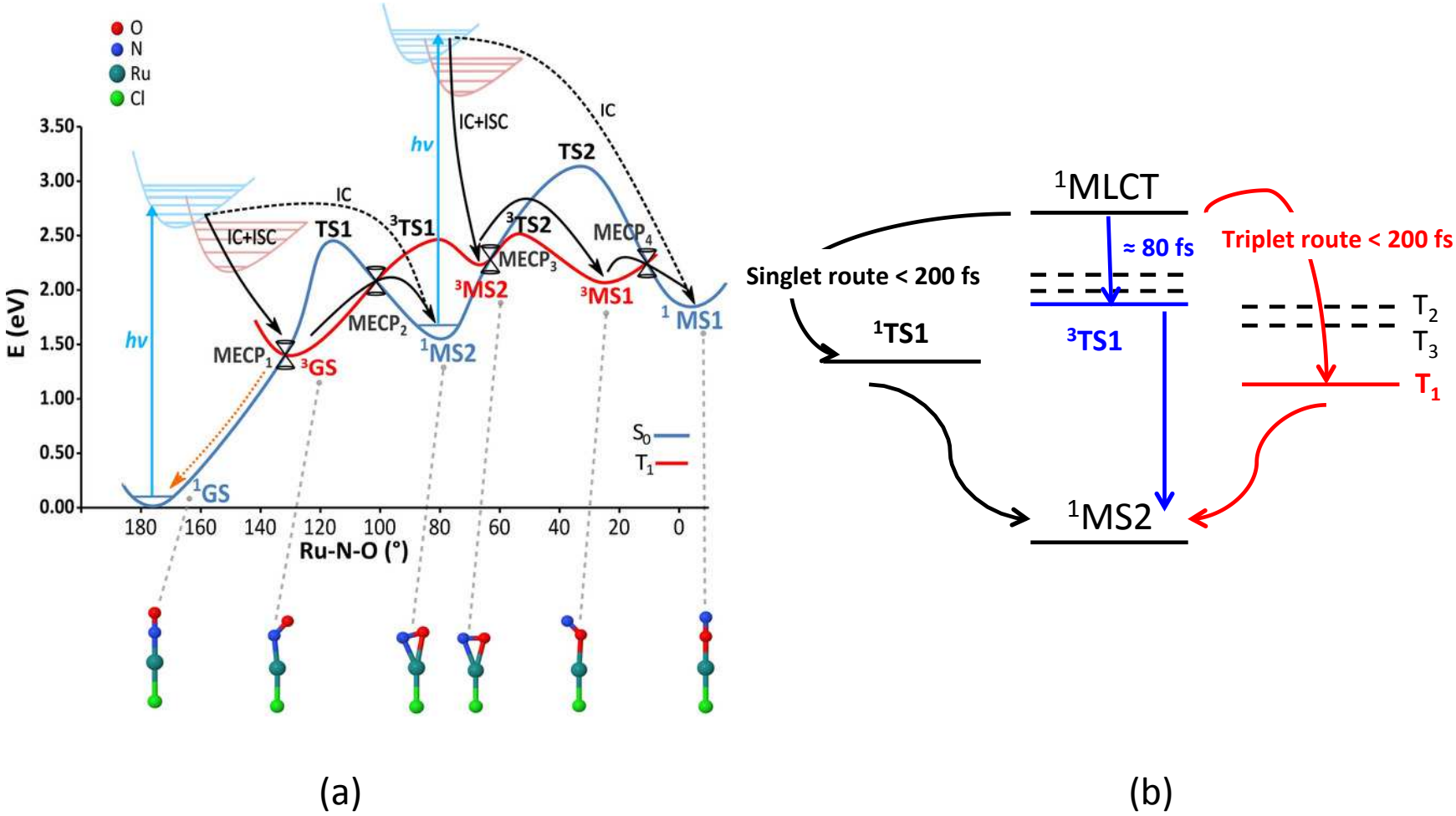

Figure 7. (a) Mechanism of $[RuCl(NO)(py)_4]^{2+}$ photoisomerization based on DFT(B3LYP) and MS-CASPT2 calculations (Adapted from Ref. 87 with the permission of the authors) (b) Three ultrafast decay pathways deduced from TSH dynamics.[67c]

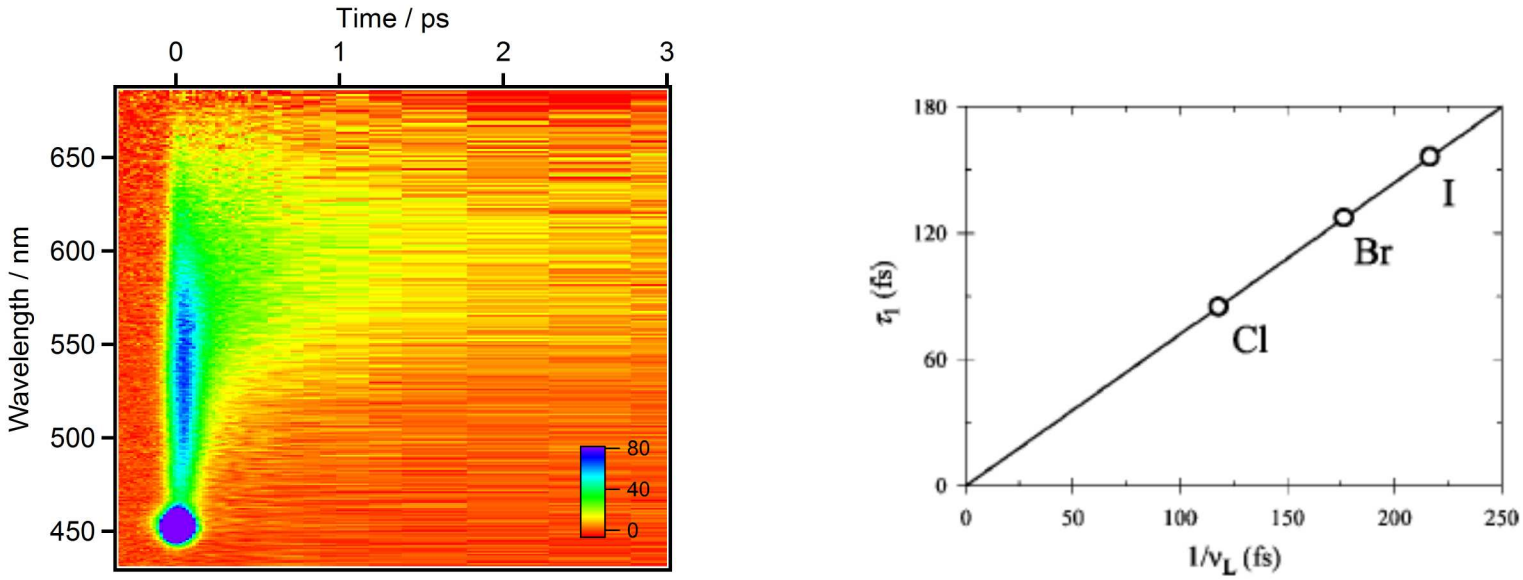

Figure 8. 2D time-resolved luminescence spectrum of [Re(Cl)$(CO)_3$(bpy)] in CH_3CN (I_{exc} = 400 nm) (a) and correlation of the ISC time-scales measured for [Re(X)$(CO)_3$(bpy)] (X=Cl, Br, I) with the vibrational period of the Re-X stretching mode in similar complexes (Adapted from Ref. 94a with the permission of the American Chemical Society).

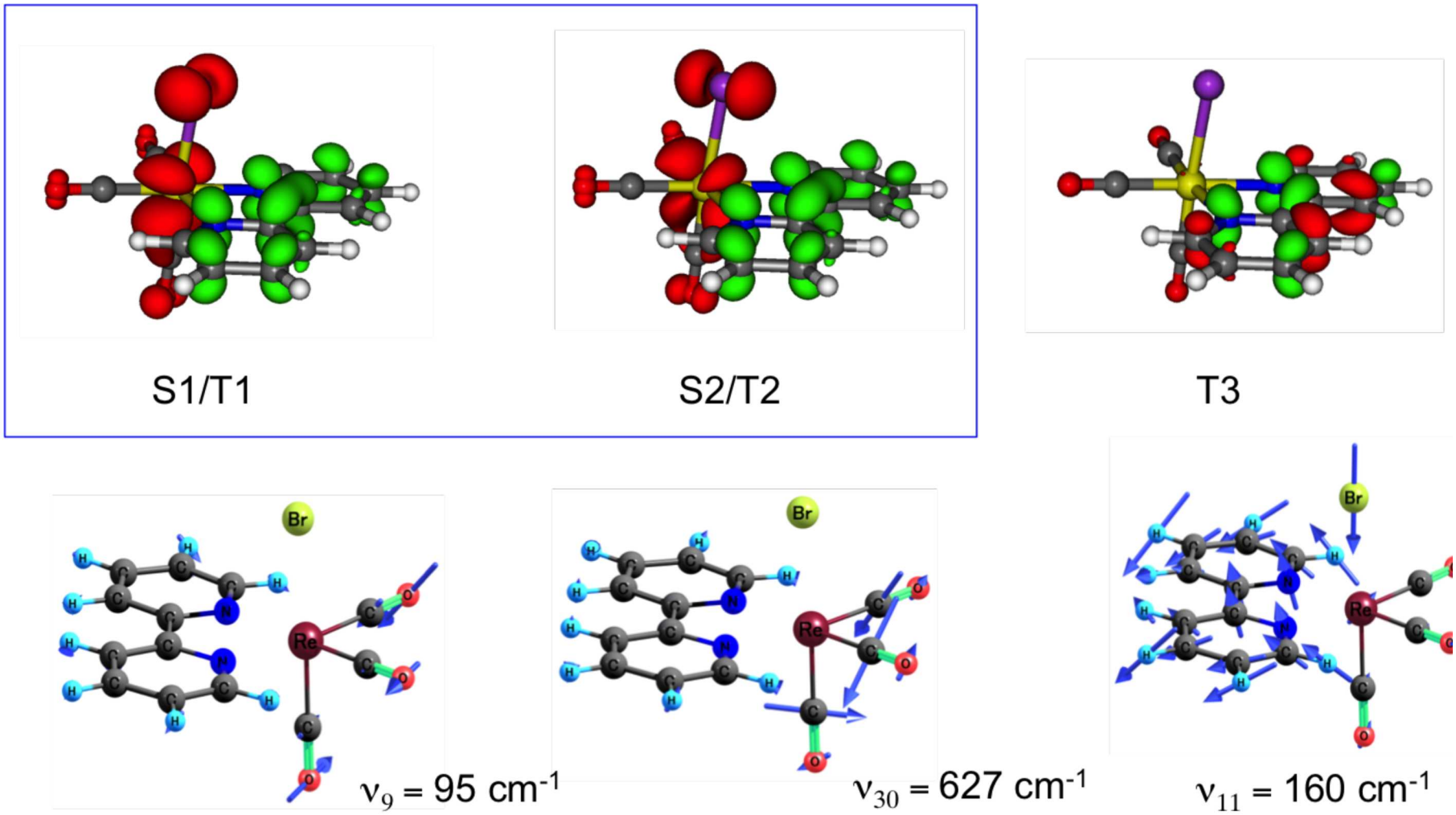

Figure 9. Differences in electronic densitiesaccompanying the $S_0 \rightarrow S_1/T_1$, $S_0 \rightarrow S_2/T_2$ and $S_0 \rightarrow T_3$ transitions in $[Re(Br)(CO)_3(bpy]$ (top) and some associated dominant symmetric tuning modes responsible for the intrastate coupling.

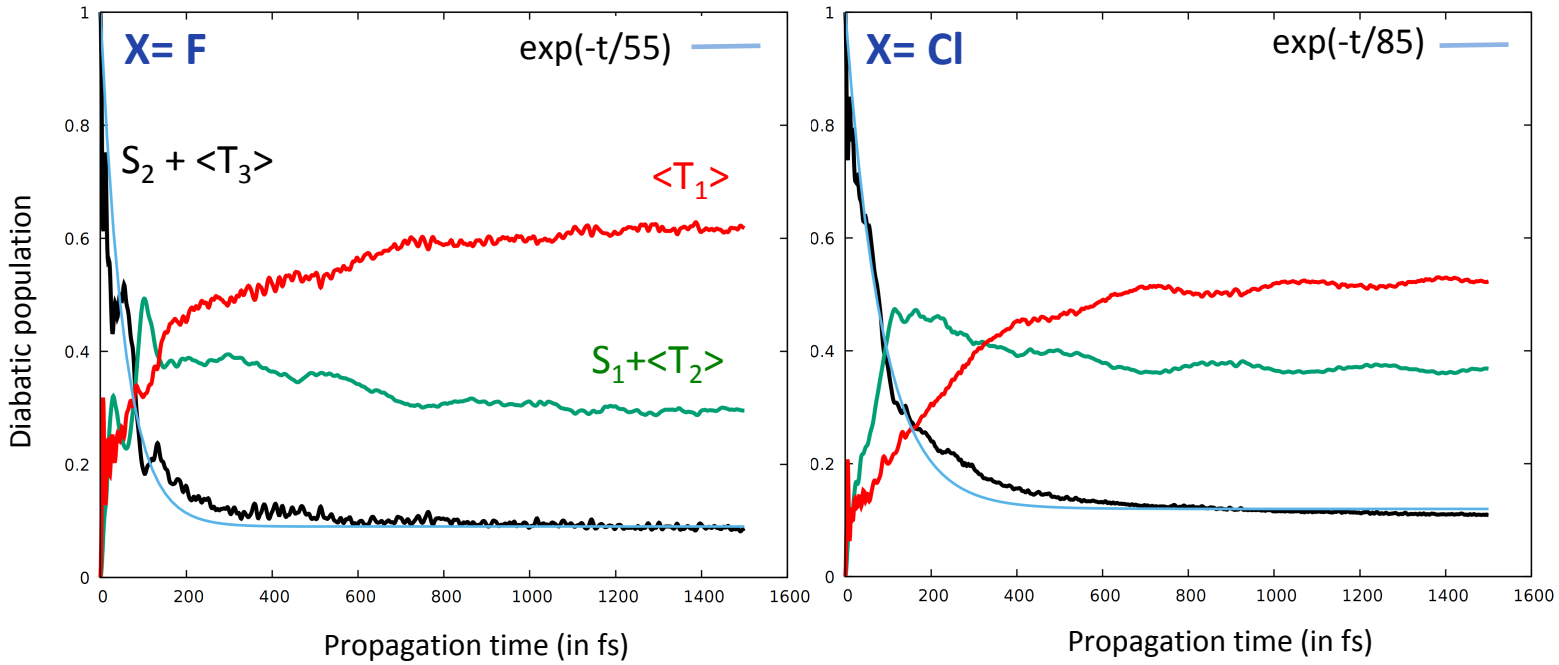

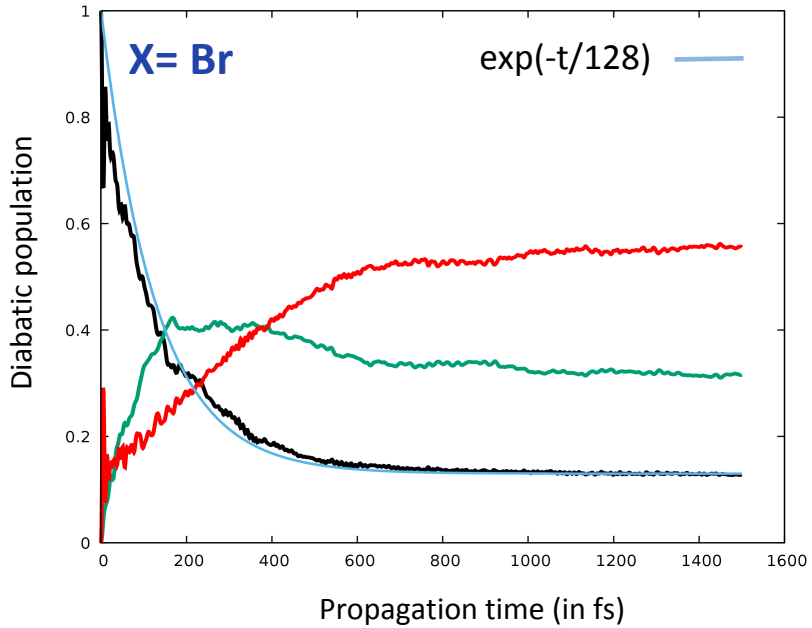

Figure 10. Time-evolution of the population of the low-lying T_3, S_2/T_2 and S_1/T_1 excited states in [Re(F)$(CO)_3$(bpy)] (a), [Re(Cl)$(CO)_3$(bpy)] (b) and [Re(Br)$(CO)_3$(bpy)] (c). For the sake of clarity the S_2/T_3 and S_1/T_2 populations are summed up. [97]

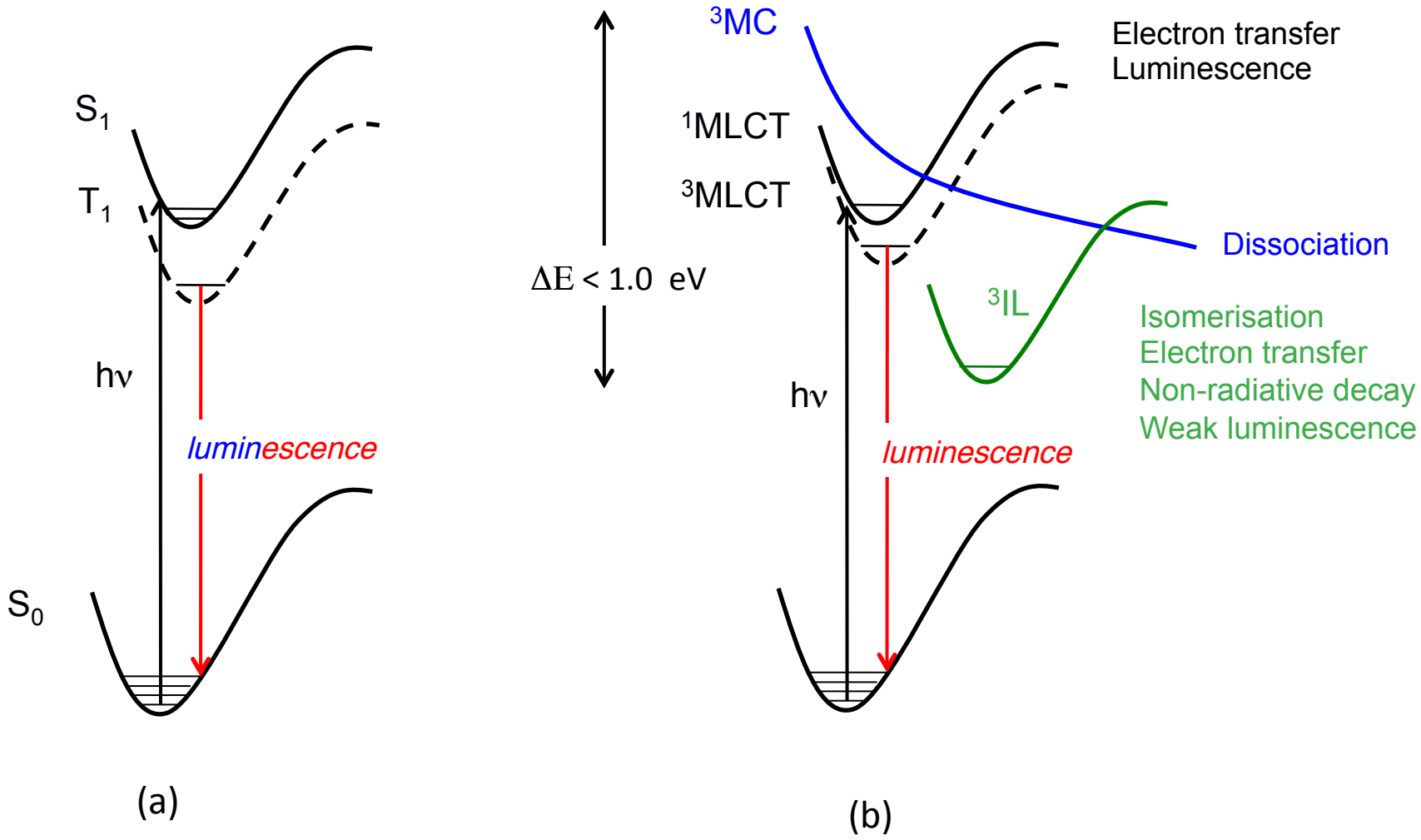

Scheme 1. (a) Luminescent decay based on the two-state model (b) Cartoon of typical radiative and non-radiative decays in coordination compounds.

CASPT2 state diagram at FC Heme-CO model complex

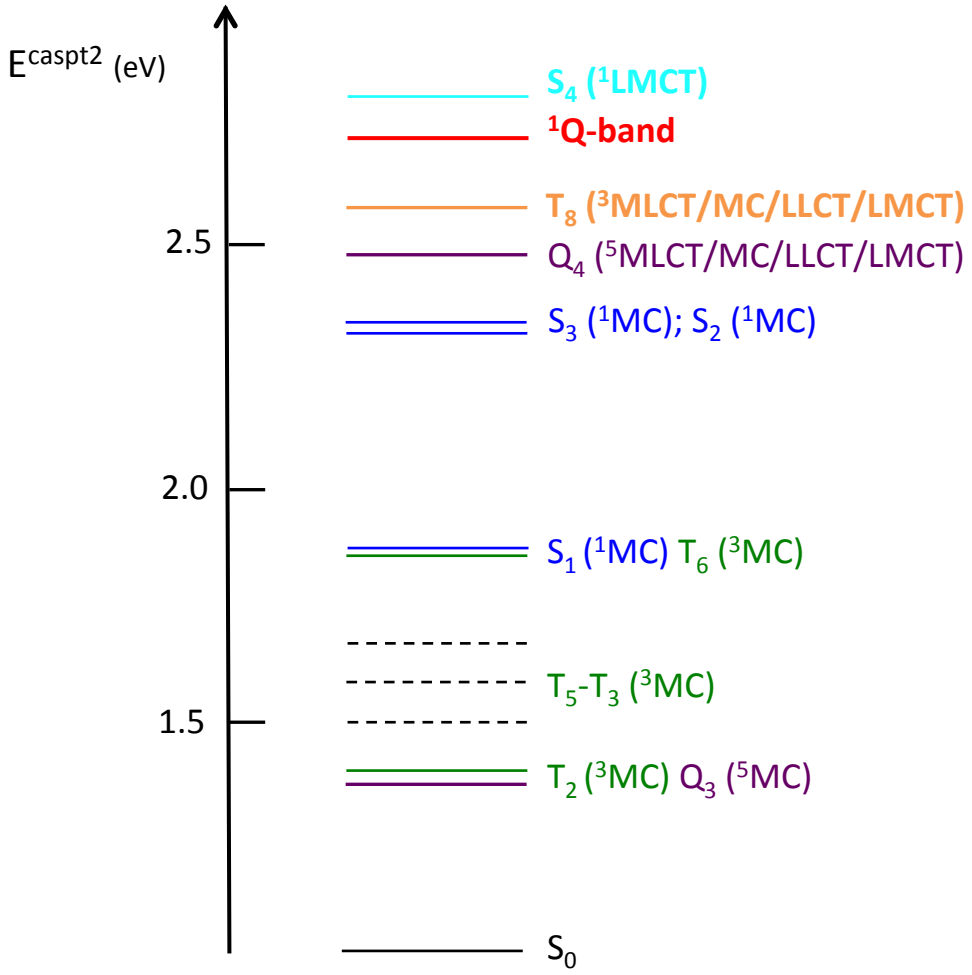

Scheme 2. CASPT2 calculated excited state diagram of the heme-CO model complex (Figure 4(b)).[52]

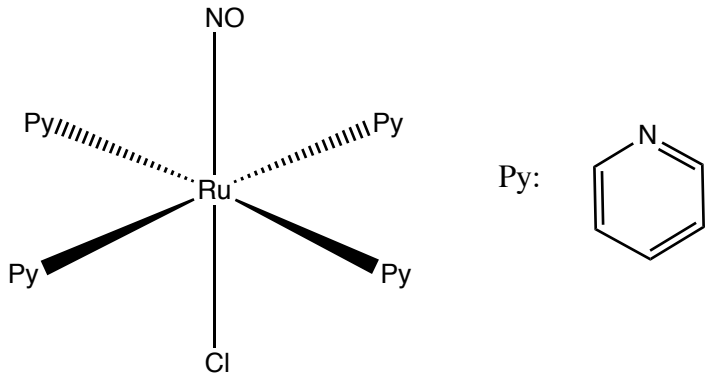

Scheme 3. Schematic structure of $[RuCl(NO)(py)_4]^{2+}$

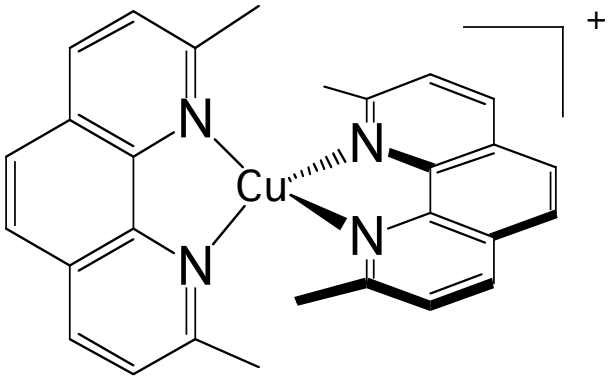

Scheme 4. Schematic structure of $[Cu(dmp)_2]^+$.

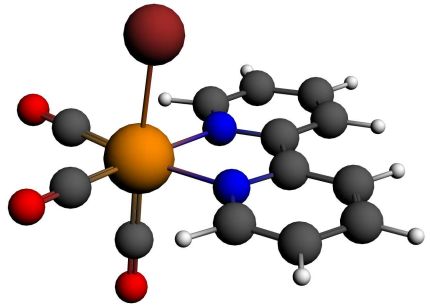

Scheme 5. Structure of the $[Re(X)(CO)_3(bpy)]$ complexes.

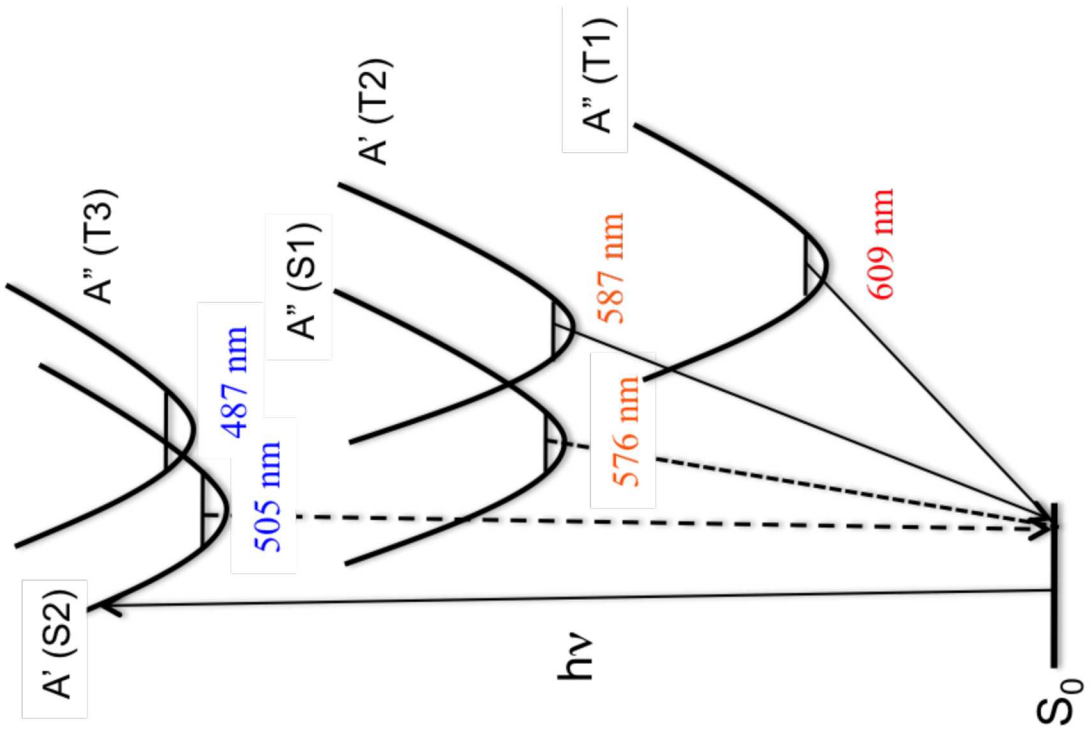

Scheme 6. Schematic representation of the potential energy curves associated to the low-lying excited states of [Re(Br)(CO)$_3$(bpy)].

Table of contents

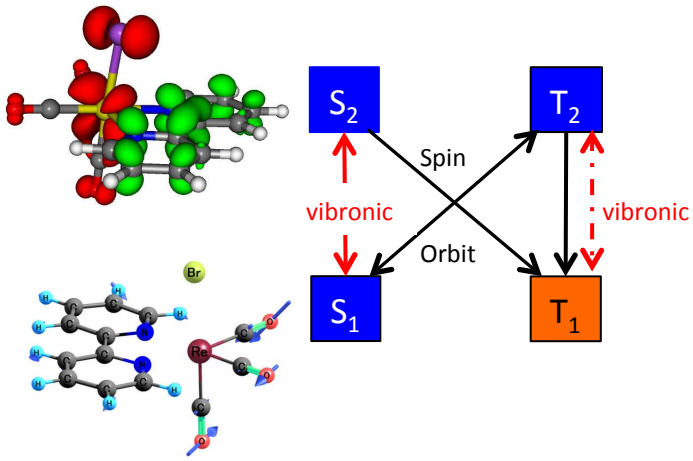

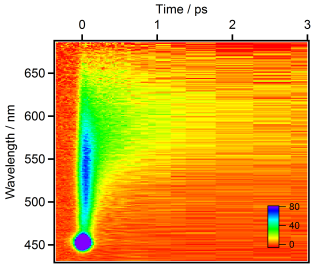

Correlation between electronic densities and active molecular vibrations drives spin-vibronic mechanism of ultrafast decays in coordination chemistry

Copyright Clearance Center RightsLink®

Help Email Support

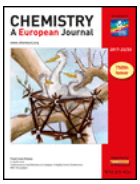

Early Relaxation Dynamics in the Photoswitchable Complex trans-[RuCl(NO)(py)4]2

Author: Leticia González, Martial Boggio-Pasqua, Francesco Talotta

Publication: Chemistry - A European Journal

Publisher: John Wiley and Sons

Date: Aug 4, 2020

© 2020 The Authors. Published by Wiley-VCH GmbH

Open Access Article

This is an open access article distributed under the terms of the Creative Commons CC BY license, which permits unrestricted use, distribution, and reproduction in any medium, provided the original work is properly cited.

You are not required to obtain permission to reuse this article.

For an understanding of what is meant by the terms of the Creative Commons License, please refer to Wiley's Open Access Terms and Conditions.

Permission is not required for this type of reuse.

Wiley offers a professional reprint service for high quality reproduction of articles from over 1400 scientific and medical journals. Wiley's reprint service offers:

- Peer reviewed research or reviews
- Tailored collections of articles
- A professional high quality finish
- Glossy journal style color covers
- Company or brand customisation
- Language translations
- Prompt turnaround times and delivery directly to your office, warehouse or congress.

Please contact our Reprints department for a quotation. Email corporatesaleseurope@wiley.com or corporatesalesusa@wiley.com or corporatesalesDE@wiley.com.

© 2020 Copyright - All Rights Reserved | Copyright Clearance Center, Inc. | Privacy statement | Terms and Conditions
Comments? We would like to hear from you. E-mail us at customercare@copyright.com

Copyright Clearance Center RightsLink®

Home | Help | Email Support | Sign in | Create Account

ACS Publications
Most Trusted. Most Cited. Most Read.

Femtosecond Fluorescence and Intersystem Crossing in Rhenium(I) Carbonyl−Bipyridine Complexes

Author: Andrea Cannizzo, Ana Maria Blanco-Rodríguez, Amal El Nahhas, et al
Publication: Journal of the American Chemical Society
Publisher: American Chemical Society
Date: Jul 1, 2008

Copyright © 2008, American Chemical Society

PERMISSION/LICENSE IS GRANTED FOR YOUR ORDER AT NO CHARGE

This type of permission/license, instead of the standard Terms & Conditions, is sent to you because no fee is being charged for your order. Please note the following:

- Permission is granted for your request in both print and electronic formats, and translations.
- If figures and/or tables were requested, they may be adapted or used in part.
- Please print this page for your records and send a copy of it to your publisher/graduate school.
- Appropriate credit for the requested material should be given as follows: "Reprinted (adapted) with permission from (COMPLETE REFERENCE CITATION). Copyright (YEAR) American Chemical Society." Insert appropriate information in place of the capitalized words.
- One-time permission is granted only for the use specified in your request. No additional uses are granted (such as derivative works or other editions). For any other uses, please submit a new request.

If credit is given to another source for the material you requested, permission must be obtained from that source.

BACK CLOSE WINDOW

© 2020 Copyright - All Rights Reserved | Copyright Clearance Center, Inc. | Privacy statement | Terms and Conditions
Comments? We would like to hear from you. E-mail us at customercare@copyright.com

Copyright Clearance Center RightsLink®

Home | Help | Email Support | Sign in | Create Account

ACS Publications
Most Trusted. Most Cited. Most Read.

Effect of tert-Butyl Functionalization on the Photoexcited Decay of a Fe(II)-N-Heterocyclic Carbene Complex

Author: Mátyás Pápai, Thomas J. Penfold, Klaus B. Møller

Publication: The Journal of Physical Chemistry C
Publisher: American Chemical Society
Date: Aug 1, 2016

Copyright © 2016, American Chemical Society

PERMISSION/LICENSE IS GRANTED FOR YOUR ORDER AT NO CHARGE

This type of permission/license, instead of the standard Terms & Conditions, is sent to you because no fee is being charged for your order. Please note the following:

- Permission is granted for your request in both print and electronic formats, and translations.
- If figures and/or tables were requested, they may be adapted or used in part.
- Please print this page for your records and send a copy of it to your publisher/graduate school.
- Appropriate credit for the requested material should be given as follows: "Reprinted (adapted) with permission from (COMPLETE REFERENCE CITATION). Copyright (YEAR) American Chemical Society." Insert appropriate information in place of the capitalized words.
- One-time permission is granted only for the use specified in your request. No additional uses are granted (such as derivative works or other editions). For any other uses, please submit a new request.

If credit is given to another source for the material you requested, permission must be obtained from that source.

BACK CLOSE WINDOW

© 2020 Copyright - All Rights Reserved | Copyright Clearance Center, Inc. | Privacy statement | Terms and Conditions
Comments? We would like to hear from you. E-mail us at customercare@copyright.com

Copyright Clearance Center RightsLink®

Home | Help | Email Support | Sign in | Create Account

ACS Publications
Most Trusted. Most Cited. Most Read.

High-Efficiency Iron Photosensitizer Explained with Quantum Wavepacket Dynamics

Author: Mátyás Pápai, György Vankó, Tamás Rozgonyi, et al

Publication: Journal of Physical Chemistry Letters
Publisher: American Chemical Society
Date: Jun 1, 2016

Copyright © 2016, American Chemical Society

PERMISSION/LICENSE IS GRANTED FOR YOUR ORDER AT NO CHARGE

This type of permission/license, instead of the standard Terms & Conditions, is sent to you because no fee is being charged for your order. Please note the following:

- Permission is granted for your request in both print and electronic formats, and translations.
- If figures and/or tables were requested, they may be adapted or used in part.
- Please print this page for your records and send a copy of it to your publisher/graduate school.
- Appropriate credit for the requested material should be given as follows: "Reprinted (adapted) with permission from (COMPLETE REFERENCE CITATION). Copyright (YEAR) American Chemical Society." Insert appropriate information in place of the capitalized words.
- One-time permission is granted only for the use specified in your request. No additional uses are granted (such as derivative works or other editions). For any other uses, please submit a new request.

If credit is given to another source for the material you requested, permission must be obtained from that source.

BACK CLOSE WINDOW

© 2020 Copyright - All Rights Reserved | Copyright Clearance Center, Inc. | Privacy statement | Terms and Conditions
Comments? We would like to hear from you. E-mail us at customercare@copyright.com